

AD-766 510

DIRECT OBSERVATION OF TRANSVERSE
STRESSES: THE TANGENTIAL STRESS GAGE

Theodore F. Stubbs, et al

Physics International Company

Prepared for:

Advanced Research Projects Agency

August 1973

DISTRIBUTED BY:

NTIS

National Technical Information Service
U. S. DEPARTMENT OF COMMERCE
5285 Port Royal Road, Springfield Va. 22151

AD 766510

Contractor: Physics International Company
Effective Date of Contract: August 22, 1972
Contract Expiration Date: October 14, 1973
Amount of Contract: \$22,015
Contract Number: H0220014
Principal Manager: T. Stubbs (415-357-4610)
Project Supervisor: F. Sauer (415-357-4610)

DIRECT OBSERVATION OF TRANSVERSE STRESSES:
THE TANGENTIAL STRESS GAGE

PIFR-393
(FINAL REPORT)

August 1973

by

T. F. Stubbs, K. D. Seifert, and R. P. Swift

Sponsored by

Advanced Research Projects Agency
ARPA Order No. 1579, Amend. 3
Program Code 2F10

DDC
RECEIVED
SEP 17 1973
REGULATED
E

The views and conclusions contained in this document are those of the authors and should not be interpreted as necessarily representing the official policies, either expressed or implied, of the Advanced Research Projects Agency or the U. S. Government.

Reproduced by
NATIONAL TECHNICAL
INFORMATION SERVICE
U S Department of Commerce
Springfield VA 22151

DISTRIBUTION STATEMENT A
Approved for public release;
Distribution Unlimited

PHYSICS INTERNATIONAL COMPANY
2700 MERCED STREET • SAN LEANDRO, CALIF. 94761 • PHONE 357-4610 (415) • TWX (910) 366-7033



UNCLASSIFIED

SECURITY CLASSIFICATION OF THIS PAGE (When Data Entered)

REPORT DOCUMENTATION PAGE		READ INSTRUCTIONS BEFORE COMPLETING FORM
1. REPORT NUMBER PIFR-393	2. GOVT ACCESSION NO.	3. RECIPIENT'S CATALOG NUMBER
4. TITLE (and Subtitle) Direct Observation of Transverse Stresses: The Tangential Stress Gage		5. TYPE OF REPORT & PERIOD COVERED Draft Final, January 14 1972 - February 14, 1973
		6. PERFORMING ORG. REPORT NUMBER PIFR-393
7. AUTHOR(s) Stubbs, Theodore F.; Seifert, Kerry D.; Swift, Robert P.		8. CONTRACT OR GRANT NUMBER(s) H0220014
9. PERFORMING ORGANIZATION NAME AND ADDRESS Physics International Company 2700 Merced Street San Leandro, California 94577		10. PROGRAM ELEMENT, PROJECT, TASK AREA & WORK UNIT NUMBERS Arpa Order No. 1579, Amend 3, Code Number 2F10
11. CONTROLLING OFFICE NAME AND ADDRESS Advanced Research Projects Agency Arlington, Virginia 20209		12. REPORT DATE August 1973
		13. NUMBER OF PAGES 73
14. MONITORING AGENCY NAME & ADDRESS (if different from Controlling Office)		15. SECURITY CLASS. (of this report) Unclassified
		15a. DECLASSIFICATION/DOWNGRADING SCHEDULE
16. DISTRIBUTION STATEMENT (of this Report) Distribution of this document is unlimited		
17. DISTRIBUTION STATEMENT (of the abstract entered in Block 20, if different from Report)		
18. SUPPLEMENTARY NOTES		
19. KEY WORDS (Continue on reverse side if necessary and identify by block number) Stress gage Tangential stress In-situ properties Rock mechanics Piezoresistive carbon		
20. ABSTRACT (Continue on reverse side if necessary and identify by block number) The ability to measure dynamic constitutive properties of geologic materials in-situ would be greatly enhanced by the existence of an accurate gage able to measure principal stresses normal to the propagation vector of a shock front. This problem has been attacked previously with moderate success and it is the objective of this work to develop and laboratory test such a device.		

DD FORM 1473
1 JAN 73

EDITION OF 1 NOV 68 IS OBSOLETE

UNCLASSIFIED

SECURITY CLASSIFICATION OF THIS PAGE (When Data Entered)

DD Form 1473: Report Documentation Page
UNCLASSIFIED

SECURITY CLASSIFICATION OF THIS PAGE(When Data Entered)

As designed, the gage consists of a piezoresistive carbon-impregnated phenolic (developed by Effects Technology, Incorporated) laminated between two 0.005-inch-thick sheets of sapphire. Electrical leads are vapor-deposited gold film. It is concluded that this gage package can adequately perform the function of directly measuring transverse stress history so long as risetimes of less than 0.5 μ s are not required.

Building upon previous work, three successive stages in the development were performed. First a design was finalized and computationally checked for equilibration time and stress level. It was determined that the stress at the active gage element would reach the correct equilibration amplitude in about 0.3 μ s and should oscillate at high frequency and low amplitude about that point.

The second stage comprised the experimental testing of the gage in uniaxial strain (triaxial stress) with peak major principal stress around 10 kbar. Three experiments were conducted: two with the gages mounted in 6061-T6 aluminum and one with the gages mounted in Westerly granite. Results were such that the gage design appeared to operate nominally.

During the third and final stage, the gage design was tested in a spherically symmetric, high explosive experiment in Westerly granite. The gages were mounted on or near the surface of a 1-foot-cube of granite with an additional 3 inches of granite backing outside of the gages. A 2-inch-diameter sphere of LX-04 was detonated at the center of the block. Not only did the gages perform as expected, but also there are indications that the gage, as designed, can perform under tensile stresses.

Contractor: Physics International Company
Effective Date of Contract: August 22, 1972
Contract Expiration Date: October 14, 1973
Amount of Contract: \$22,015
Contract Number: H0220014
Principal Manager: T. Stubbs (415-357-4610)
Project Supervisor: F. Sauer (415-357-4610)

DIRECT OBSERVATION OF TRANSVERSE STRESSES:
THE TANGENTIAL STRESS GAGE
PIFR-393
(FINAL REPORT)

August 1973

by

T. F. Stubbs, K. D. Seifert, and R. P. Swift

Sponsored by

Advanced Research Projects Agency
ARPA Order No. 1579, Amend. 3
Program Code 2F10

The views and conclusions contained in this document are those of the authors and should not be interpreted as necessarily representing the official policies, either expressed or implied, of the Advanced Research Projects Agency or the U. S. Government.

Preparing Agency

Physics International Company
2700 Merced Street
San Leandro, California 94577

ABSTRACT

The ability to measure dynamic constitutive properties of geologic materials in-situ would be greatly enhanced by the existence of an accurate gage able to measure principal stresses normal to the propagation vector of a shock front. This problem has been attacked previously with moderate success and it was the objective of this work to develop and laboratory test such a device.

As designed, the gage consists of a piezoresistive carbon-impregnated phenolic (developed by Effects Technology, Incorporated) laminated between two 0.005-inch-thick sheets of sapphire. Electrical leads are vapor-deposited gold film. It is concluded that this gage package can adequately perform the function of directly measuring transverse stress history so long as risetimes of less than 0.5 μ s are not required.

Building upon previous work, three successive stages in the development were performed. First a design was finalized and computationally checked for equilibration time and stress level. It was determined that the stress at the active gage element would reach the correct equilibration amplitude in about 0.3 μ s and should oscillate at high frequency and low amplitude about that point.

The second stage comprised the experimental testing of the gage in uniaxial strain (triaxial stress) with peak major principal stress around 10 kbar. Three experiments were conducted: two

with the gages mounted in 6061-T6 aluminum and one with the gages mounted in Westerly granite. Results were such that the gage design appeared to operate nominally.

During the third and final stage, the gage design was tested in a spherically symmetric, high explosive experiment in Westerly granite. The gages were mounted on or near the surface of a 1-foot-cube of granite with an additional 3 inches of granite backing outside of the gages. A 2-inch-diameter sphere of LX-04 was detonated at the center of the block. Not only did the gages perform as expected, but also there are indications that the gage, as designed, can perform under tensile stresses.

ACKNOWLEDGEMENTS

The authors extend their heartfelt thanks to Walter J. Naumann of Effects Technology, Inc. for his advice during the formative stages and throughout this program and for the assembly of the carbon element gage packages used in this work.

Our appreciation is also extended to Mr. John Atkins of the Bureau of Mines for his many helpful suggestions.

This research was supported by the Advanced Research Projects Agency of the Department of Defense and was monitored by the Bureau of Mines under Contract No. H0220014.

CONTENTS

	<u>Page</u>
SECTION 1 INTRODUCTION	1
1.1 Background	1
1.2 Objectives	2
SECTION 2 GAGE DESIGN AND CALCULATIONS	5
2.1 Background	5
2.2 Design	6
2.3 Estimate Equilibration Time and Stress	10
SECTION 3 UNIAXIAL STRAIN SHOCK EXPERIMENTS	19
3.1 Procedures	19
3.2 Results	26
3.3 Summary	35
SECTION 4 SHOCK EXPERIMENT IN SPHERICAL SYMMETRY	37
4.1 Procedures	37
4.2 Results	41
4.3 Discussion	47
SECTION 5 TECHNICAL REPORT SUMMARY	51
5.1 Technical Problems	51
5.2 General Methodology	52
5.3 Technical Results	53
5.4 DOD Implications	55
REFERENCES	
APPENDIX ANOMOLIES SEEN IN MANGANIN GAGES	

Preceding page blank

ILLUSTRATIONS

<u>Figure</u>		<u>Page</u>
1	Shock and Transverse Mode Gage Geometry	7
2	Greatly Simplified Shock Profiles in Transverse Gage Package	8
3	Carbon Element (Upper) and Manganin Element (Lower) Stress Transducers	11
4	Zoning for One-Dimensional Estimate of Gage Equilibration Time and Stress	12
5	Stress History Calculated at Centerline of Figure 3	14
6	Stress History of a Point Within Aluminum Block	15
7	Velocity History of Aluminum-Epoxy Interface	16
8	Stress Profile Throughout Aluminum Stress Gage Package at 0.300 μ s	17
9	Experimental Configuration for All Uniaxial Strain Experiments	20
10	Aluminum Targets in Pre- and Post-Assembled Conditions Showing Gage Placement and Milled Gage Slots	22
11	Simplified Schematic of Electronic Circuit	23
12	Recorded Data from First Uniaxial Strain Test in Aluminum	27
13	Reduced Data From First Uniaxial Strain Experiment in Aluminum	27

Preceding page blank

ILLUSTRATIONS (cont.)

<u>Figure</u>		<u>Page</u>
14	Recorded Data from Second Uniaxial Strain Test in Aluminum	28
15	Reduced Data from Second Uniaxial Strain Experiment in Aluminum	29
16	ETI Carbon Stress Gage Calibration	31
17	Recorded Data from Uniaxial Strain Experiment in Westerly Granite	32
18	Reduced Data from Uniaxial Strain Experiment in Westerly Granite	33
19	Preassembly "Exploded" View of Granite Block for Spherically Symmetric Experiment	38
20	Split Backing Plate (Side c) Exposing Slot to Admit Tangential Gage	39
21	Final View of Granite Block Immediately Prior to Experimentation	40
22	Recorded Data from Spherical Experiment in Westerly Granite (Positive Resistance Change is up)	42
23	Reduced Data from Spherical Experiment in Westerly Granite	44
24	Stress Histories and Paths Derived from Figure 23	46

SECTION 1 INTRODUCTION

1.1 BACKGROUND

Although the dynamic constitutive properties of samples of geologic materials may be determined to a fair degree of precision in the laboratory, it has long been recognized that these measurements may be considerably at variance with the in-situ values (Reference 1). There are several reasons for this difference. One is that the sample may not be representative of the fractured mass. Another is that the in-situ state of lithostatic stress of the region from which the sample is taken may not be known. Clearly, some technique of measuring simultaneously the states of stress and of strain of the material in-situ is required.

Long term stress-strain creep has been measured with varying degrees of success by overcoring and borehole deformation. For the dynamic situation, most of the suggestions have centered around inverting the equations of motion using measured stress and velocity histories. As the gages measuring stress and motion must, in this case, move with the material, a Lagrangian formulation of the equations is indicated. Fowles and Williams (Reference 2) suggested one such formulation requiring the measurement of stress and momentum phase velocities. The gage system requirements to obtain the desired properties were extensively investigated in an earlier report (Reference 3) with the conclusion that this particular formalism did not, in spherical geometry, admit

the accurate calculation of tangential stress from radial measurements only. It was further concluded that the development of a gage to measure tangential stress directly was of paramount priority. The efforts to develop such a device comprise the main body of this report.

Concurrent with the above investigation, Grady (Reference 4), using a more general expression of the equations of motion for the same purpose, concluded that, at least for the unloading portion of the stress wave, it was possible to obtain a reasonably accurate calculation of tangential stress from measurements of radial velocity and stress only. It would thus appear that development of a tangential stress gage is necessary only to obtain the loading portion of the wave. However, it must be noted that Grady quite reasonably took waveforms from several gage stations to obtain his result, while severe restrictions were imposed on the previous work by limiting the analysis to two gage stations and degrading the computer generated data to conform to that expected from a field experiment. A tangential gage may well be needed in a field system to measure in-situ properties; in any case, such a device would serve as confirmation of the calculations and vice versa.

1.2 OBJECTIVES

Godfrey and McKay (Reference 5) discuss the results of preliminary attempts to develop a deviatoric gage. Although their success was marginal, they pointed the direction in which to proceed by recognizing the mitigating effects. In their work the active elements were single manganin wires of circular cross section mounted in layers of epoxy. Each epoxy layer was normal to the stress expected to be measured. This is standard procedure

for measuring stress normal to the shock front however, the tangential transducer was, by necessity, mounted in a layer along which the shock propagated. A Mach stem was created within this epoxy layer due to the impedance mismatch between it and the material in which the stress was to be measured, leading to a very high pulse at the outset of the tangential stress record. It was pointed out that the elimination of the Mach stem, the elimination of its effects, or both, should lead to a well-behaved gage.

The objectives of this work were the design, construction, and testing of a gage that is economical to produce, simple to use, and that mitigates both the Mach stem and its effects.

SECTION 2

GAGE DESIGN AND CALCULATIONS

2.1 BACKGROUND

Observations of Reference 5 lead to the conclusion that the effects of the Mach stem are of short duration and localized to the shock front. The ambiguities of the inclusion of the Mach spike in a gage record may be mitigated by increasing the gage response time to such an extent that signals having frequency content at or above that of the Mach spike are not recorded. This is not a wholly satisfactory solution when the waveform during loading and unloading is required and the frequency content of these portions of the waveform cannot be recorded. In uniaxial dynamic strain tests (e.g., projectile or gas gun experiments) one is usually interested in one or more equilibrium stress levels which have been reached through a shock loading or unloading process. The frequency response of the gage is unimportant for this application (so long as it is sufficiently high to clearly reach and maintain the equilibration state) while elimination of large and spurious transients is of prime importance.

For the transverse mode gage let "t" be the dimension of the active gage element parallel to the propagation vector of the shock, t^2 the area of the element normal to the stress the element is to sense, and w the dimension of the gage normal to both

Preceding page blank

t and d (Figure 1). In the work of Reference 1 the gage element had a shock aspect ratio t/w of 1.0 (a circular cross section manganin wire). It was pointed out that by increasing the aspect ratio, the gage risetime would proportionately increase; however, the spatially small effect of the Mach stem would be lost. The design of the active portion of the gage is based upon such reasoning.

2.2 DESIGN

The magnitude of the stress in the Mach stem may be reduced or the stem itself effectively eliminated by laminating the gage element between thin layers of a material having a higher sound speed than the test specimen. This may be seen in Figure 2 where it is assumed that a uniaxial stress wave of magnitude σ_0 is propagating through the specimen at velocity U_s .

Both a compressional (P) and a shear wave (S) are shed from the shock front into the epoxy, bonding the gage package into the specimen. Any compressional signal generated in the high-velocity laminate material will lose its shock front identity and become part of the "outrunning" signal since it is postulated that the P-wave velocity for this material is greater than U_s . The full characterization of the shock front is in two S-wave fronts in the high-velocity laminate. Reflecting from the lower boundary of the laminate will be both S and P waves, the reflected P waves also joining the outrunning energy. Transmitted into the epoxy surrounding the gage element will be the S and P waves generated in the epoxy by the S waves in the laminate. By these mechanisms a substantial fraction of the energy in the shock front may be "trapped" in the laminate and excluded from creating a Mach stem.

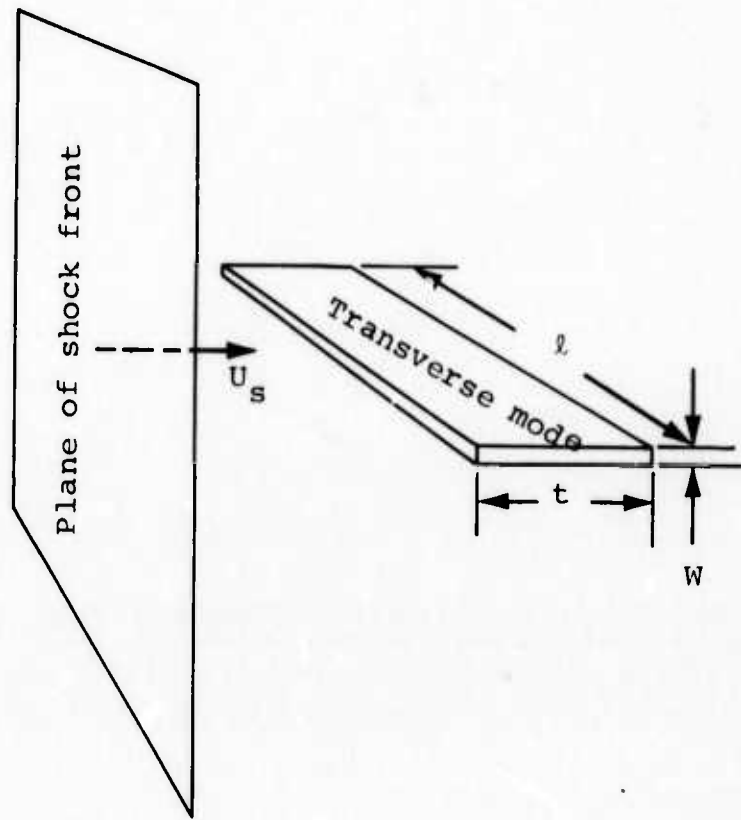


Figure 1 Shock and transverse mode gage geometry.

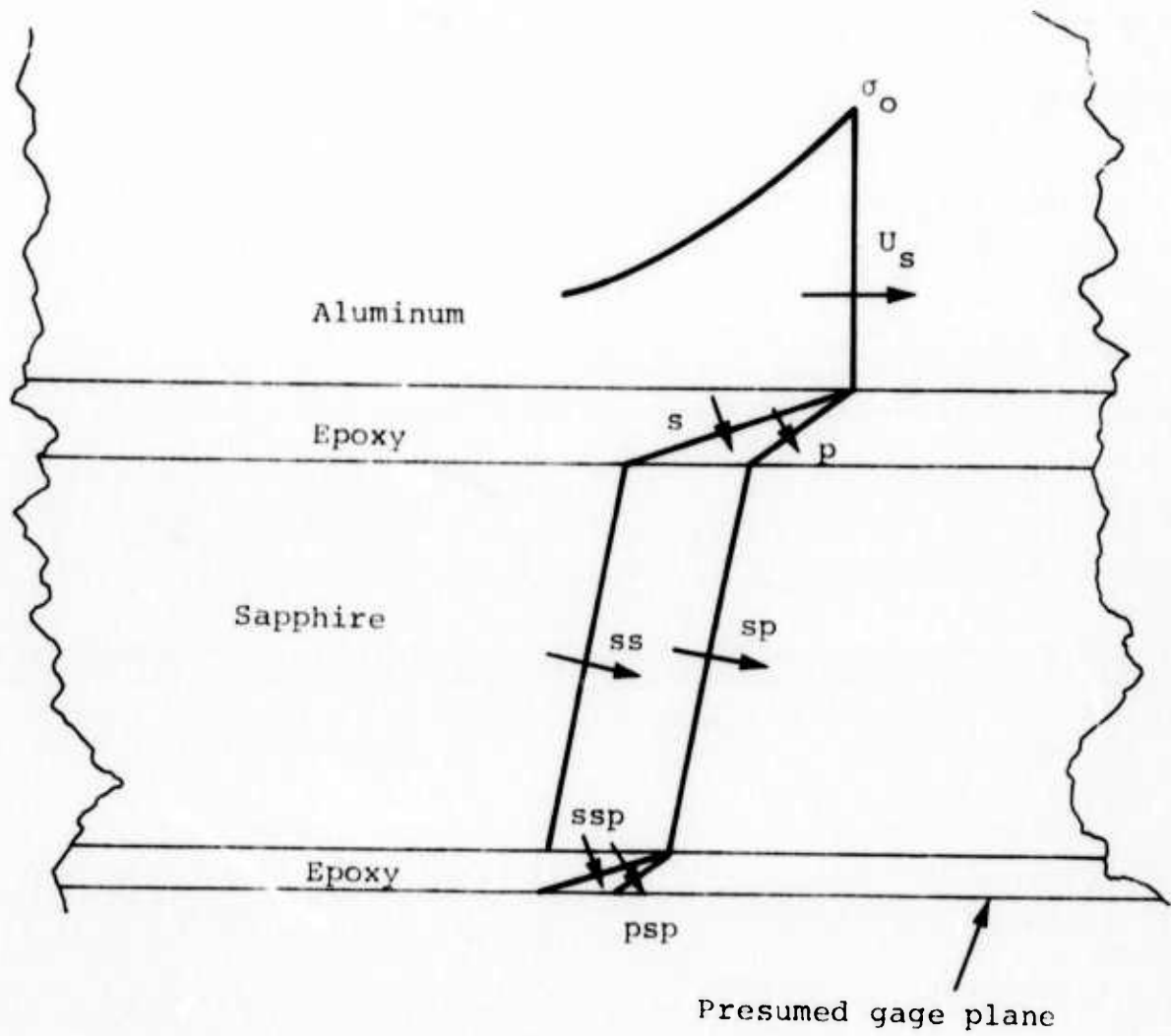


Figure 2 Greatly simplified shock profiles in transverse gage package.

Equilibration time of the gage will be whatever is required for the system to settle to the sudden application of a uniform stress, σ_0 , plus the time required for the "trapped" energy in the laminate to dissipate. The first of these equilibration times is amenable to a one-dimensional calculation while the second is not. The third factor contributing to the risetime of the gage is its width, adding a minimum time of $\tau = t/c$ where c is the shock velocity in the sample.

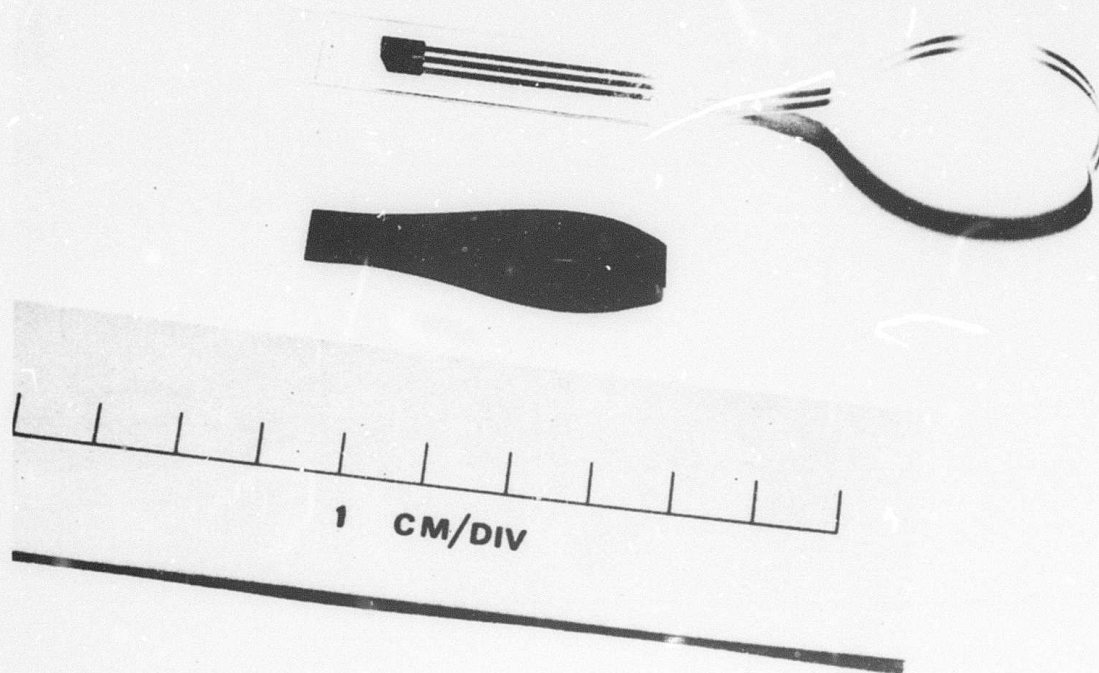
Several active element materials were considered as candidates for this work. Manganin is a reliable material with very small hysteresis; it is, however, somewhat insensitive, having a gage stress coefficient of around 400 kbar Ω_0/Ω . Ytterbium is highly sensitive and was used in the work immediately preceding this. One drawback to this material is that it has relatively low resistivity, requiring either a fairly large element or one of questionable ruggedness to obtain the desired resistance for impedance matching of the recording electronics. Further, ytterbium displays a pronounced hysteresis upon unloading, taking a permanent resistance offset when released back to zero stress. This hysteresis has not been investigated adequately for the material to be used as a standard for both loading and unloading. A third element is carbon (actually a carbon-impregnated phenolic resin) developed by Effects Technology, Incorporated (ETI, Reference 6). Its sensitivity lies between that of manganin and ytterbium: it is reliable, rugged, and has high resistance, allowing the creation of a small element having the required resistance. Hysteresis of this material is not known in detail; however, there is some evidence that the loading and unloading paths in stress-strain space are slightly different, with no permanent offset in resistance occurring. The carbon piezoresistance element was chosen for the transverse gage transducer.

Figure 3 shows one such complete carbon gage assembly and an imperfect view of a manganin gage which was used as a control. It is seen that there are three leads plated to the carbon element. Following plating of the gold leads, the element was trimmed so that the resistance from the center conductor to either of the outer conductors was close to 50 ohms. Thus, in theory, this element could act as two independent gages. Caution dictated that only one side of an element be used until it was determined that the design was a viable one; the third gas gun experiment employed both sides of the elements as independent gages as did the high-explosive test in spherical geometry. No difficulty was experienced on the gas gun test while the spherical shot indicated late time gage failure via the center lead. The true cause of this failure has not been determined.

2.3 ESTIMATE EQUILIBRATION TIME AND STRESS

As commented above, the problem of equilibrating to a step input in stress has a straightforward solution if one neglects the "trapped" two-dimensional stress waves. Equilibration in the tangential mode gage is different from that in the radial mode in that stress is applied on both sides of the gage simultaneously, in effect, making the gage element lie in a plane of symmetry. A simple one-dimensional calculation was performed in which the area of interest was a rigid boundary. The geometry of this computation is shown in Figure 4.

The sample material modeled was 2024 aluminum bounded below by a 1-mil-thick epoxy layer. Next, a 5-mil layer of the high-impedance laminate (sapphire) was followed by another 1-mil layer of epoxy. This last layer represented the active gage element and was bounded by a rigid wall. A special non-reflecting (transmitting) boundary was imposed on the upper surface of the aluminum to preclude reflections from this surface of any disturbance created in the gage region. The aluminum was pre-loaded to a uniform stress of 6.06 kbar, with no particle velocity in any zone.



(73-3-3)

Figure 3 Carbon element (upper) and manganin element (lower) stress transducers.

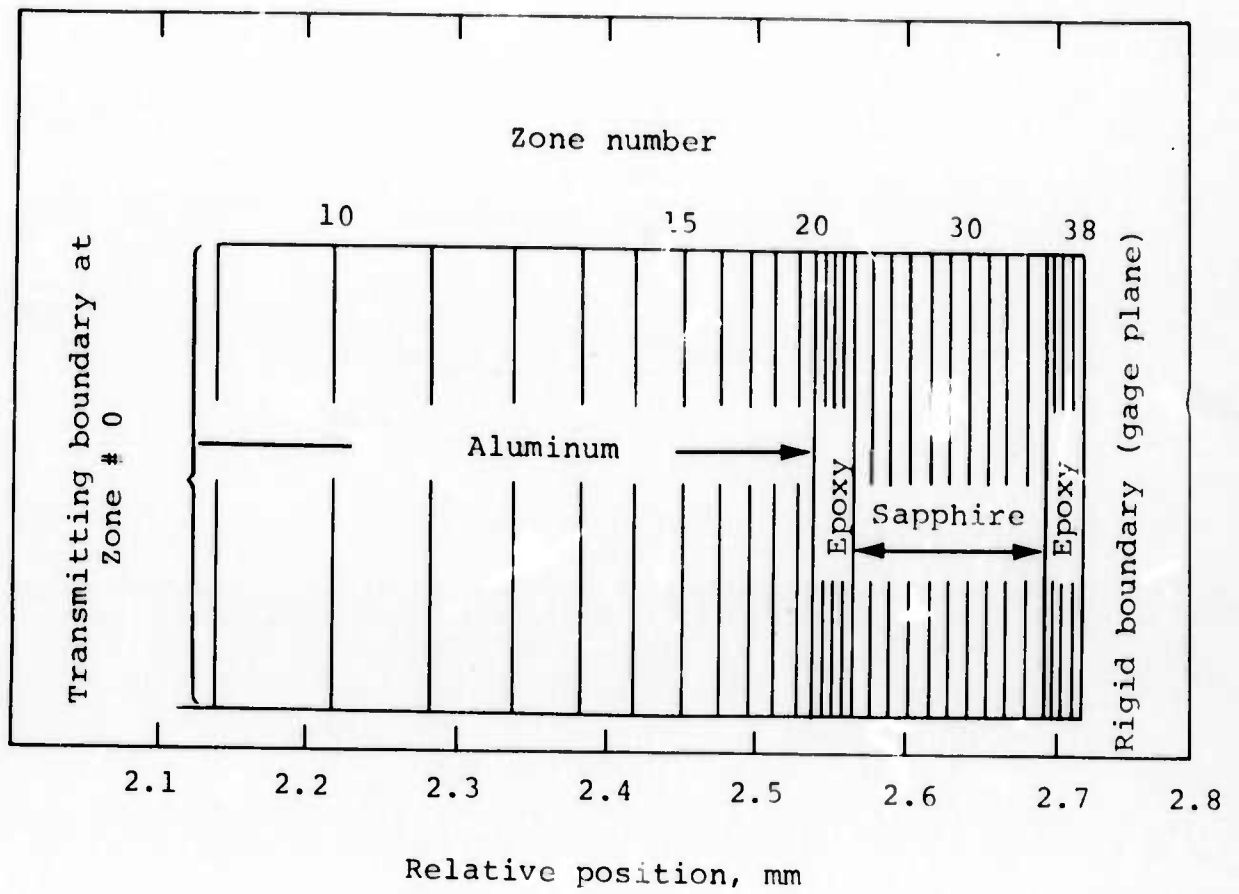


Figure 4 Zoning for one-dimensional estimate of gage equilibration time and stress.

Figure 5 shows the time history of the stress at the gage location. The stress rises to nearly the desired level in about 100 ns while the full value is reached and locked in at about 300 ns. Major oscillations result from reflections in the sapphire while minor ones are due to reflections in the epoxy layers. Figure 6 shows a stress history within the aluminum block. Again, for the first 200 ns, the stress is not the initial value; however, by about 200 ns, the aluminum is oscillating about the final equilibrium value. The velocity of the epoxy-aluminum interface is displayed in Figure 7. The conclusions above are again borne out: an oscillatory equilibration is achieved within about 300 ns.

Finally, a snapshot of the stress profile existing throughout the model at 300 ns is shown in Figure 8. The wave front is progressing toward the transmitting boundary on the left. To conserve computer time (and hence funds) the zoning on the left was made quite coarse. As all information was transmitted from right to left, this had no deleterious effect on the conclusions. The region of interest (positions greater than 0.23 cm on Figure 4) was, of course, finely zoned.

TANGENTIAL STRESS EQUILIBRATION

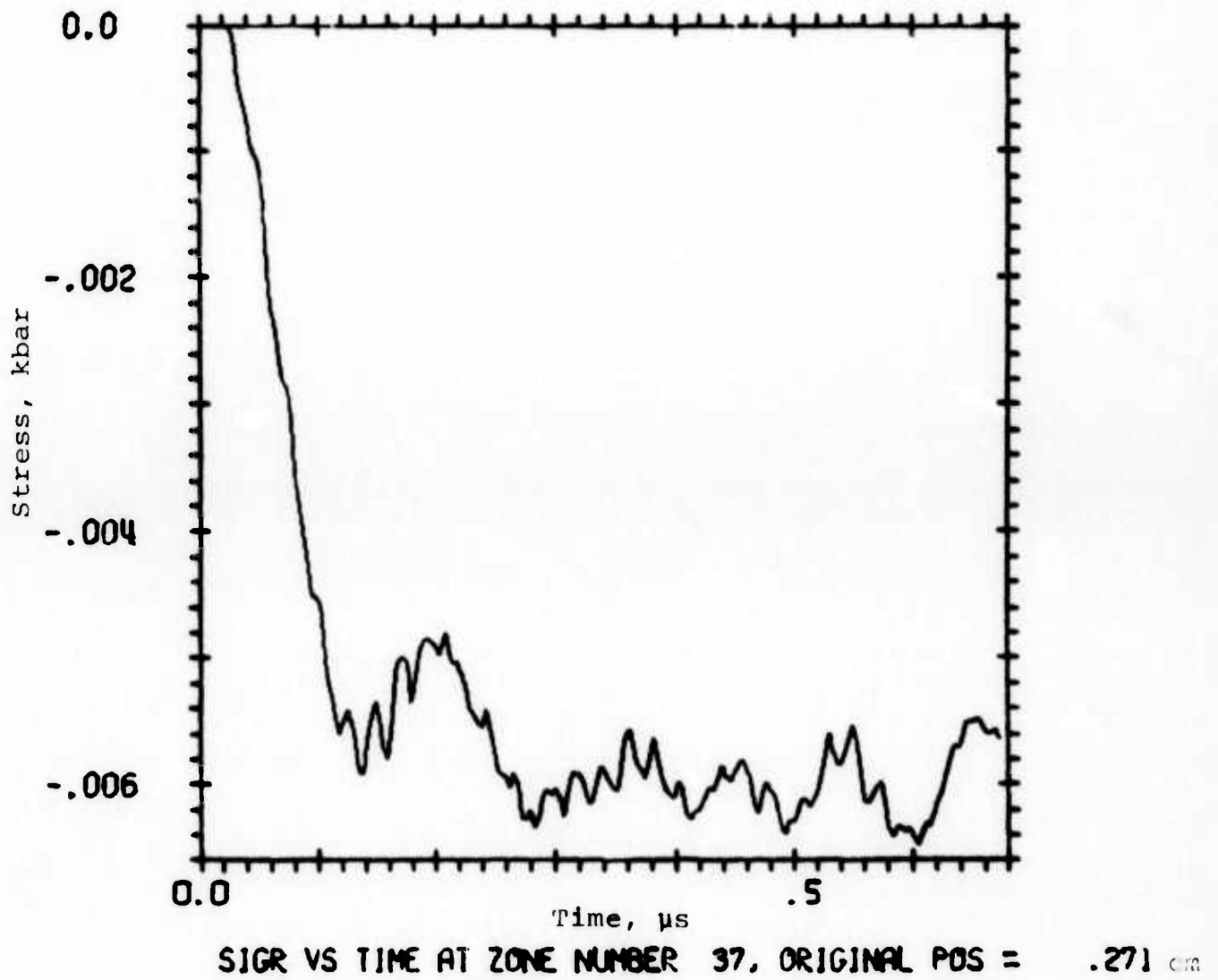


Figure 5 Stress history calculated at centerline of Figure 3.

TANGENTIAL STRESS EQUILIBRATION

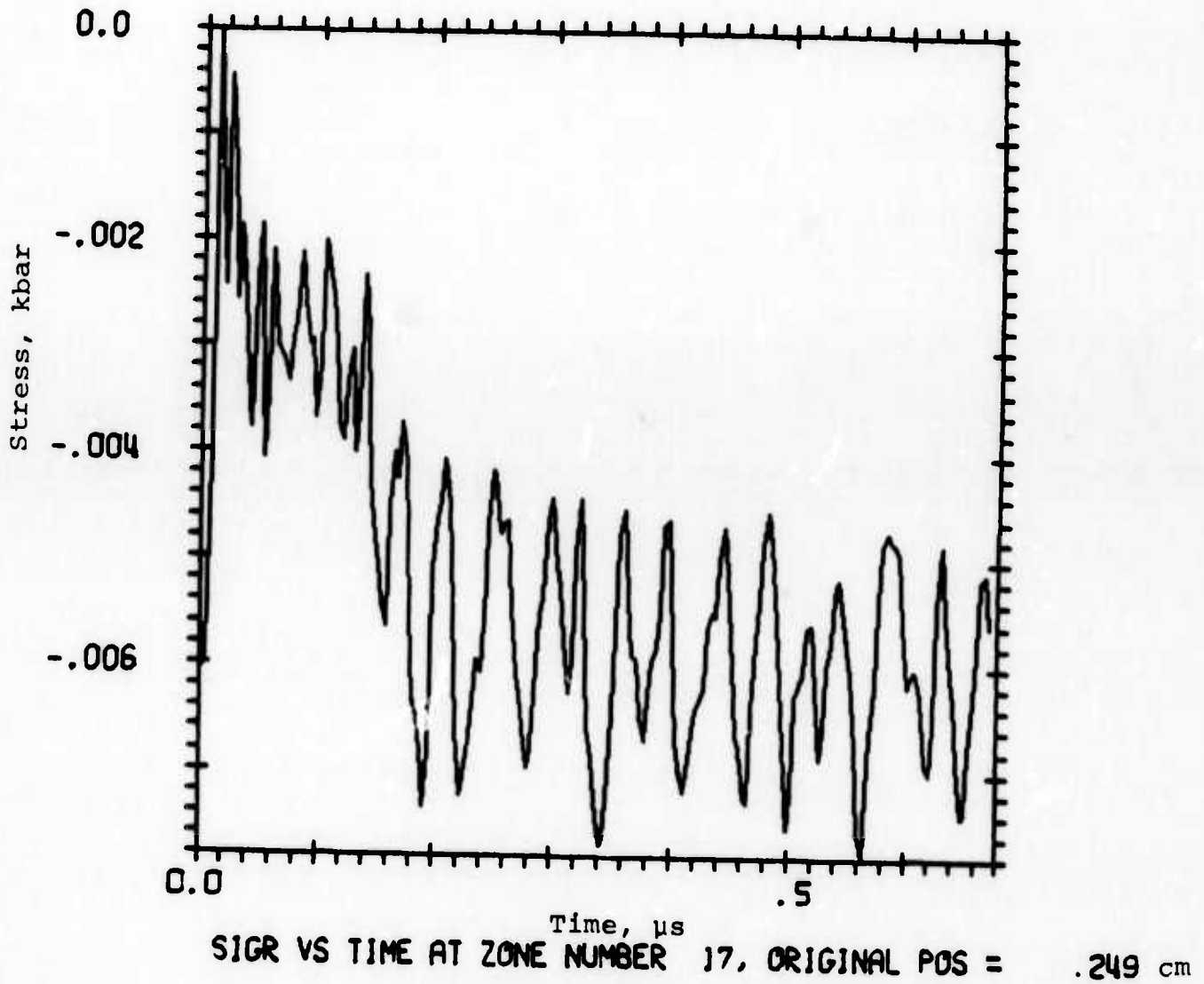


Figure 6 Stress history of a point within aluminum block.

TANGENTIAL STRESS EQUILIBRATION

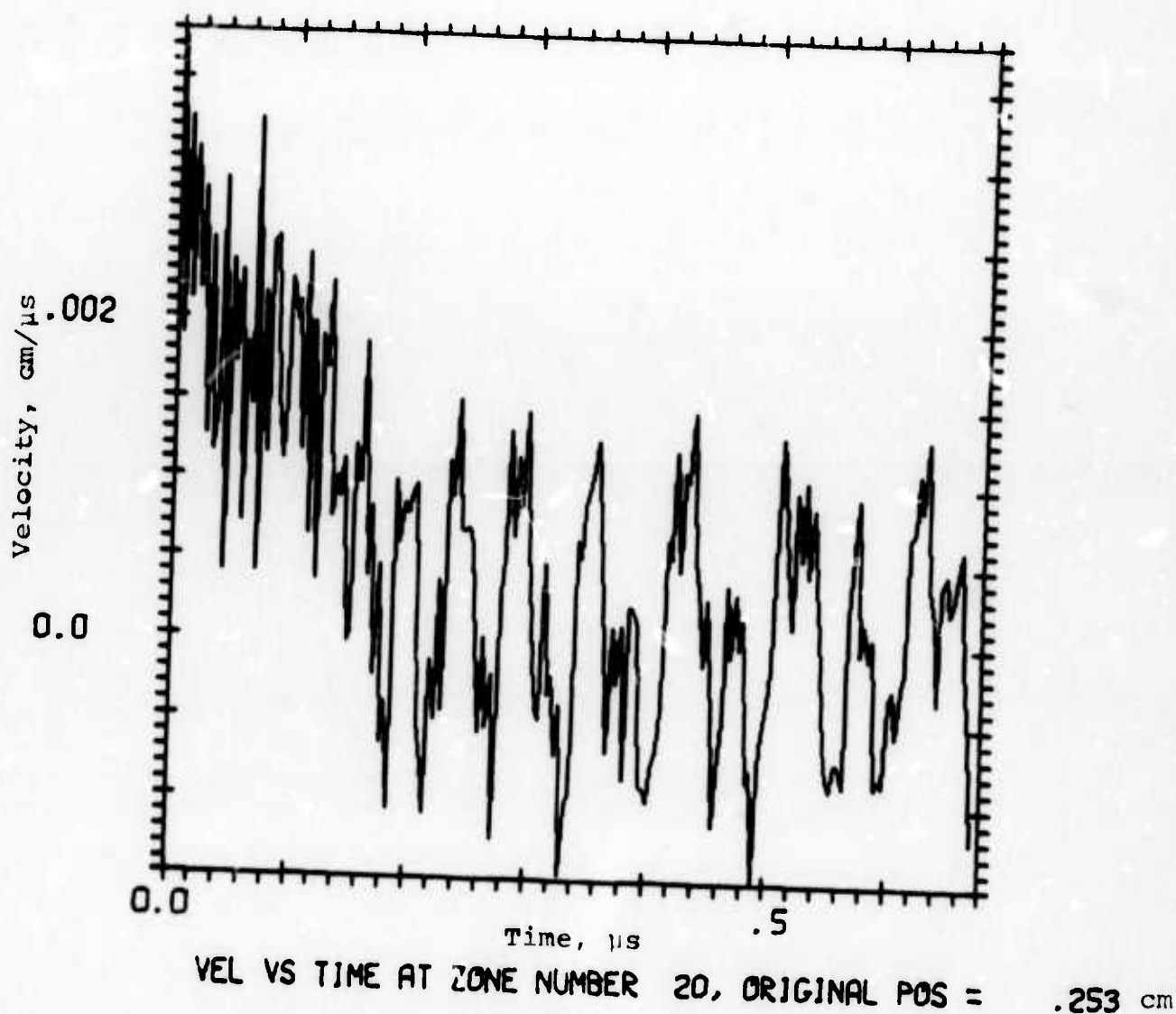


Figure 7 Velocity history of aluminum-epoxy interface.

TANGENTIAL STRESS EQUILIBRATION

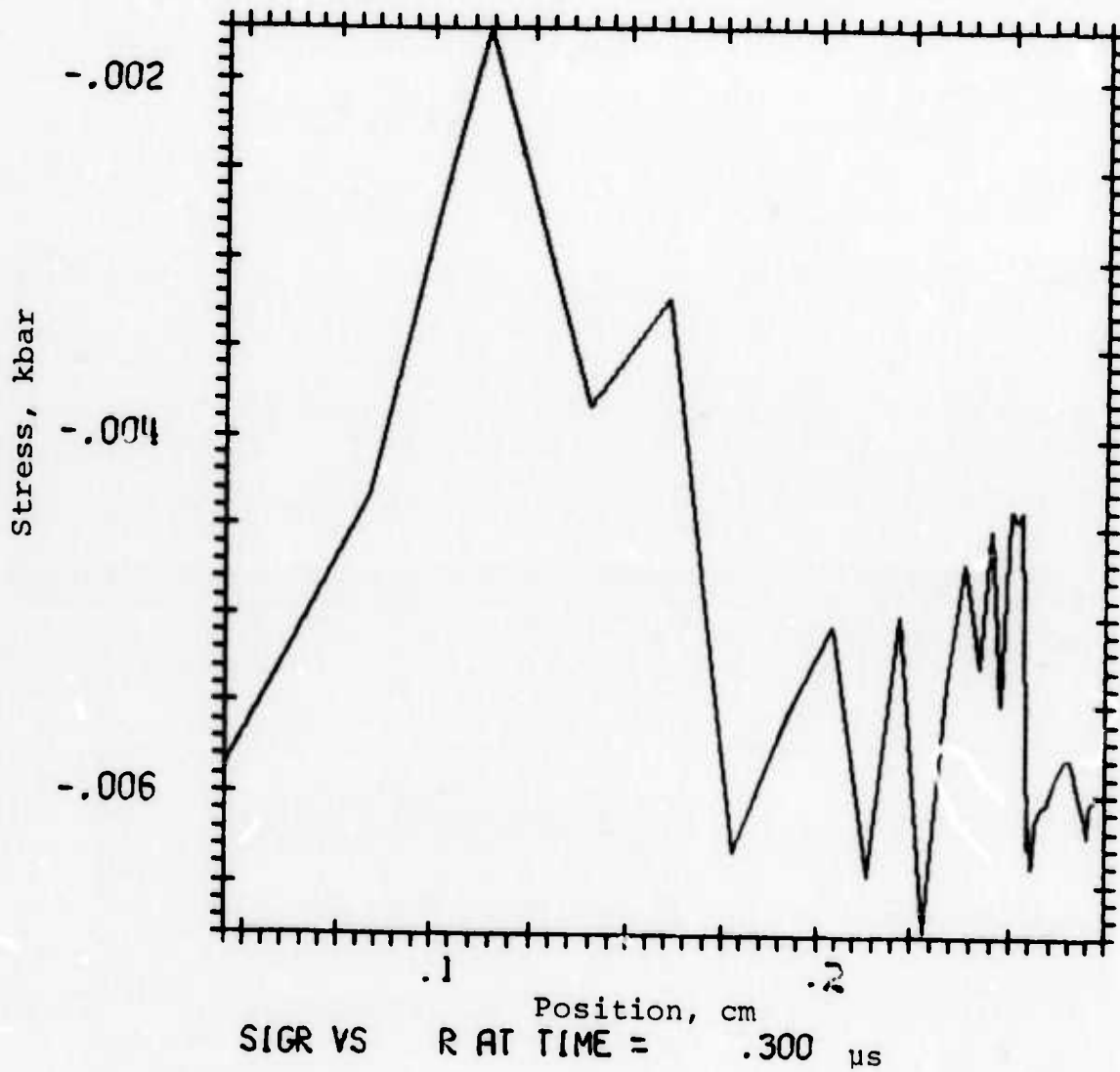


Figure 8 Stress profile throughout aluminum stress gage package at 0.300 μ s.

SECTION 3

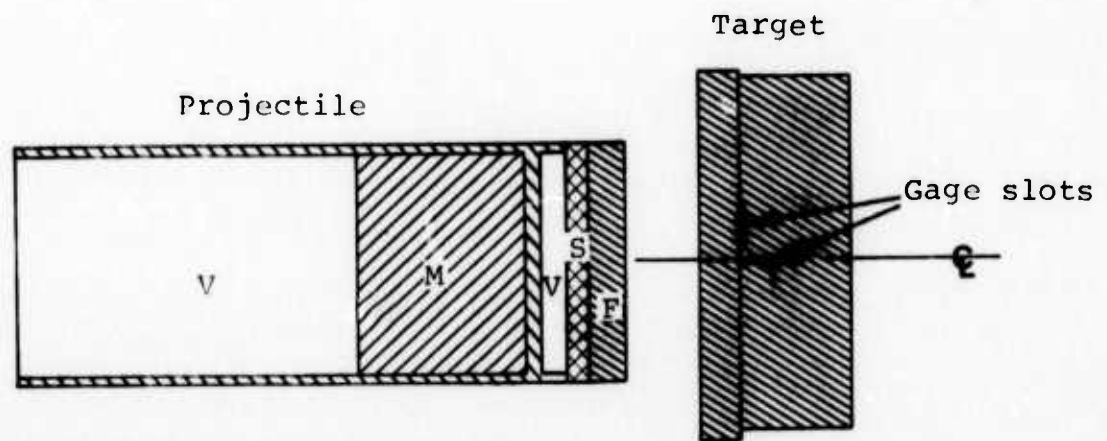
UNIAXIAL STRAIN SHOCK EXPERIMENTS

3.1 PROCEDURES

The Physics International 4-inch light gas gun was used to project a flat flyer plate against a target in which have been imbedded the gages to be studied. In all experiments reported here, the flyer plate and target were of the same material: two experiments used 6061-T6 aluminum and the third test used Westerly granite. These materials were chosen because they have been extensively studied previously and have yield stresses the same order of magnitude or greater than the maximum principal stress expected to be attained in any of the tests. This should result in a definitive test of the gage.

Figure 9 shows the basic experimental layout while Figure 10 shows the aluminum target in its finished and pre-assembly conditions. It will be noted that the flyer plate was backed by syntactic foam (hollow glass spheres in a resin matrix). This was to prevent the release wave in the target from unloading all the way to zero stress. Investigation into the hysteretic behavior of the carbon elements used in these experiments has been rudimentary and it was felt that further work was in order. A piezoresistive material having only very little hysteresis (manganin) was mounted in the axial mode in addition to one of the carbon gages. Although the sensitivity of manganin is nearly an order of magnitude below that of the carbon material, any

Preceding page blank



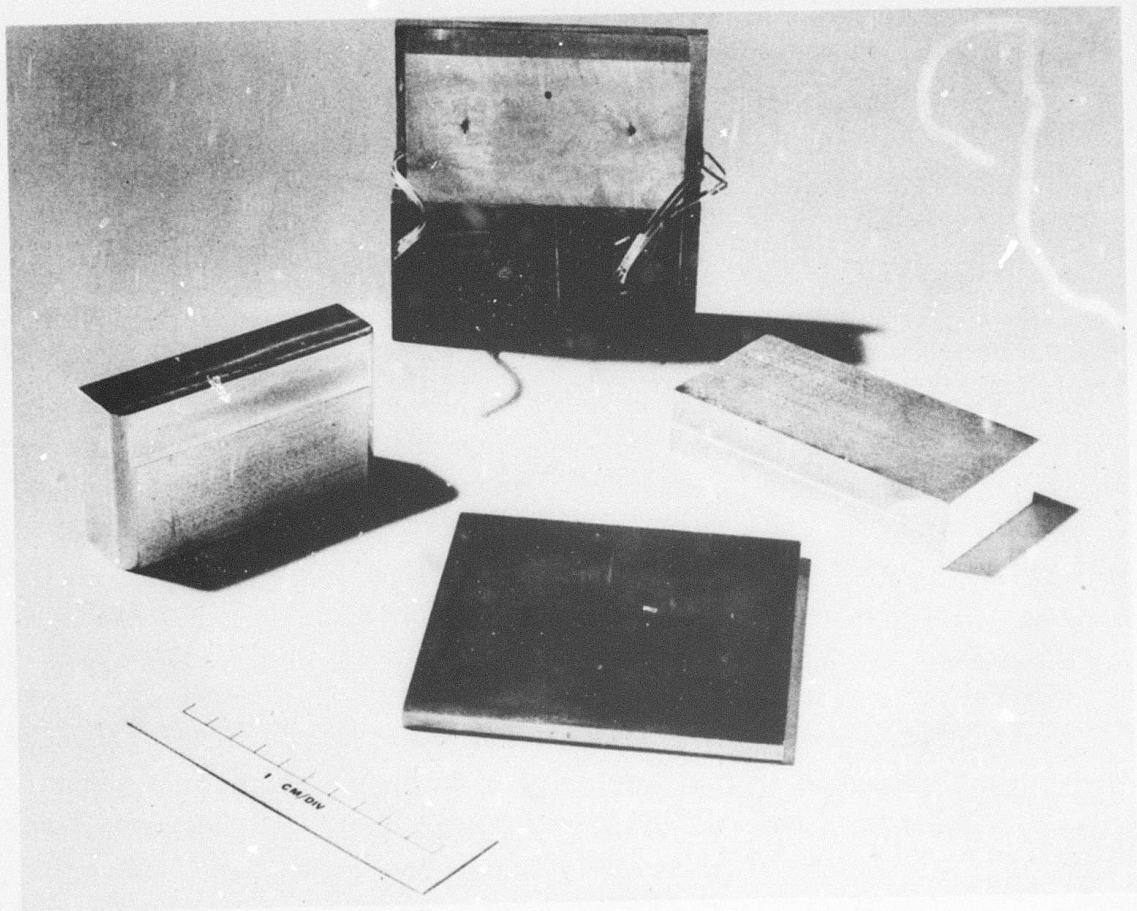
- F - flyer plate (target material)
- S - syntactic foam
- V - void
- M - mass to obtain proper projectile velocity

Gas gun experiment geometry (no scale)

Figure 9 Experimental configuration for all uniaxial strain experiments.

marked hysteresis in the carbon element upon release to some non-zero stress should be apparent when compared to the manganin gage response. Naumann (Reference 6) claims the carbon gages return to their initial resistance upon release to zero stress but show some indication of hysteresis in the path followed to reach zero stress.

As seen in Figure 10, slots about 0.012 inch deep and $\frac{1}{8}$ inch wide were milled into the target pieces to admit the gage packages. The shock propagation vector was normal to the axial mode gages and in the plane of the transverse mode transducers. Although the contact surfaces between flyer plate and target were lapped flat to a high tolerance and positioned carefully pre-shot, it was impossible to prevent some tilt between the two from occurring during the experiment. To measure and allow for this tilt, four small coaxial cables acted as pin switches penetrating the target on the circumference of a 3.75-inch-diameter circle, the center of which lay on the axis of the projectile (Figure 10). During fabrication these pins were allowed to protrude beyond the target and in the final phase were lapped to be precisely coincident with the target surface. TTL compatible voltage was impressed across the center conductor to the grounded outer sheath of each pin; as the flyer plate made contact and shorted the pins, a unique voltage for each pin was displayed on an oscilloscope. Thus the timing and position of contact between the flyer plate and target could be determined accurately. For the experiment using granite, the leading surface of the flyer plate was lightly aluminized to ensure electrical contact. The tilt pins served an additional function. All of the oscilloscopes recording shock data were triggered by the discharge of the first tilt pin to be shorted.



(73-3-4)

Figure 10 Aluminum targets in pre- and post-assembled conditions showing gage placement and milled gage slots.

Each gage formed the resistance of one leg of a Wheatstone bridge, as indicated below (Figure 11).

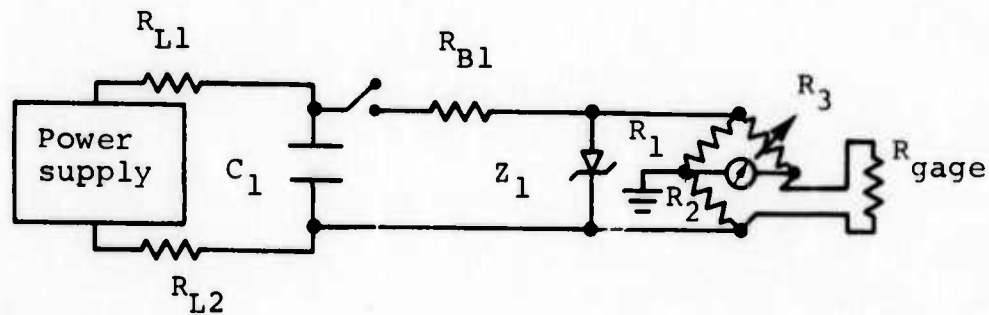


Figure 11 Simplified schematic of electronic circuit.

Capacitor C_1 was charged to a voltage substantially greater than that desired across the bridge to ensure that the decay time of the circuit upon discharge was very much greater than the time during which data were to be obtained. Ballast resistor R_{B1} served to drop the voltage to nearly that desired while the zener diode Z_1 held the voltage constant at the level required.

For the two aluminum experiments the bridges used were symmetric, that is $R_1 = R_2$. If the bridge is balanced under the condition that $R_{\text{gage}} = R_0$, then when $R_{\text{gage}} \rightarrow R_0 + \Delta R$ the voltage read at the indicator is V and is given by

$$\frac{V}{V_0} = \frac{1}{2} \frac{\frac{\Delta R}{R_0}}{2 + \frac{\Delta R}{R_0}} \quad (1)$$

Here, V_0 is the supply voltage impressed across the bridge. Equation 1 assumes that the indicator (oscilloscope) resistance is essentially infinite. Clearly, knowledge of V_0 and R_0 and measurement of V leads to the resistance change ΔR (presumably due to stress change of the gage element).

A second method of determining ΔR as a function of V is by direct pre-shot calibration. The bridge is balanced with the gage installed using a small voltage source instead of the power supply (to protect the gage from inadvertent overheating). The gage is then replaced with a variable resistance and the voltage deflection of the oscilloscope trace from the balance condition noted as a function of resistance about the value of the gage. For this, the power supply is used as in the actual experiment. This has the advantages of directly calibrating the entire system, including all unknowns (except for the gage itself), and in particular any nonlinearity that may exist in the oscilloscope amplifier. This technique was used for the second aluminum experiment and the uniaxial granite shot.

The stress level is then obtained from $\Delta R/R_0$ by the following relationships:

1. For the manganese elements

$$\sigma = K \frac{\Delta R}{R_0}$$

$$K = 400 \text{ kbar} \quad (2)$$

and

2. For the carbon elements

$$\sigma = - \frac{\Delta R}{R_0} \left[26.8 + \frac{\Delta R}{R_0} \left(21.0 + 287 \frac{\Delta R}{R_0} \right) \right] \text{ kbar} \quad (3)$$

It has been stated that K may vary by as much as 25 percent depending upon the loading rate (Reference 7). Consistency of the data of Swift (Reference 8) and those generated here along with the Hugoniot data indicates that the uncertainty is substantially less.

Naumann (Reference 6) indicates that Equation 3 for the carbon element gages is accurate to 6.5 percent. This error includes not only gage-to-gage variations, but also instrumentation errors in the calibration experiments.

The power supply to the bridge was a large capacitor bank which was discharged and decayed very slowly in comparison to the time duration of the experiment. It was triggered about 30 μ s prior to contact between the flyer plate and target. The trigger for this event was a fifth coaxial pin penetrating the target and protruding toward the flyer plate a distance set by the projectile velocity and the above delay time. Power was allowed on the bridge for a total time of about 100 μ s, after which the capacitor bank was shorted.

The velocity of the projectile was monitored by three small fiberoptic light pipes. Half of the fibers in a given pipe transmitted light from a source and the other half received reflected light and excited a photomultiplier. The pipes were accurately spaced along the muzzle end of the gas gun and as a reflecting portion of the projectile passed a light pipe, the resulting signal was recorded. Pressure in the breech of the gas gun and the mass of the projectile were adjusted to yield the desired muzzle velocity.

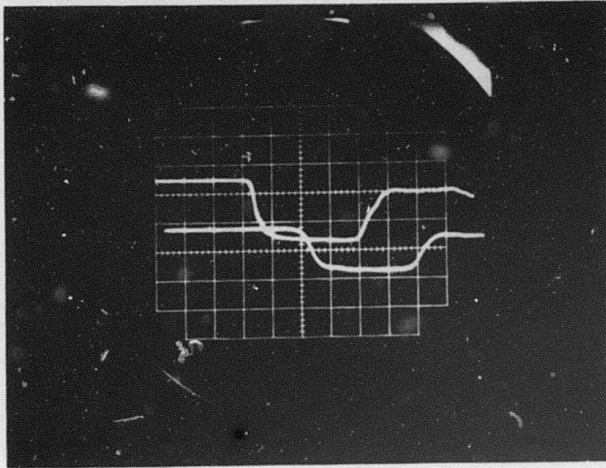
3.2 RESULTS

3.2.1 Aluminum Samples. The recorded data from the first shot are shown in Figure 12 and the reduced data in Figure 13. The manganin gage on this test was dead pre-shot. Data reduction for this shot proceeded through the inversion of Equation 1 and the use of Equation 3. Reduced data from the second test in aluminum are displayed in Figure 15 with the associated oscilloscope traces appearing as Figure 14. Here it appears as if the carbon axial-mode gage was misbehaving; the peak of the loading stress is about 20 percent in excess of both the increased value for the manganin gage and the calculated value from the shock and projectile velocities. Secondly, the carbon axial gage unloads to a value substantially below that of the transverse mode gage. ETI noted that there had been some difficulty in bonding the elements to the highly polished sapphire substrate. A lack of proper bonding is a strong candidate for the cause of the anomalous behavior. This can be eliminated in future applications by not allowing the final polish on the sapphire substrates.

As a result of the anomalous behavior, the entire system was resistance-calibrated post-shot as described in Section 3.1. Use of the bridge Equation 1 was abandoned for this test and complete reliance on the resistance calibration was made.

The rise and general character of the manganin gage are somewhat peculiar and will be discussed later in Appendix A.

Because of the rather substantial risetime of the transverse mode gage (about 0.5 μ s to equilibrate to the peak stress), the only datum one can, with confidence, derive from these tests is the



	<u>Upper</u>	<u>Lower</u>
	Radial	Trans
Gage	0.512	0.512 μs /cm
Sweep rate	1.05	1.00 V/cm
Amplitude	53.0	51.5 volts
Bridge voltage	50.7	50.6 ohms
Gage resistance		

Figure 12 Recorded data from first uniaxial strain test in aluminum.

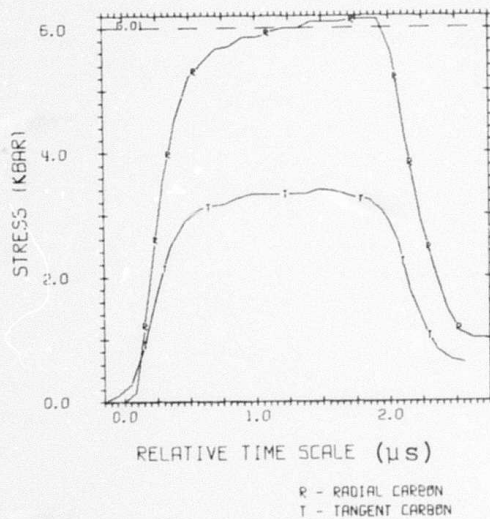
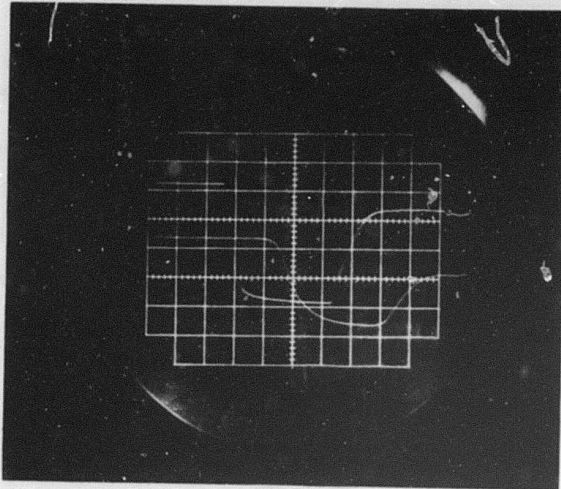
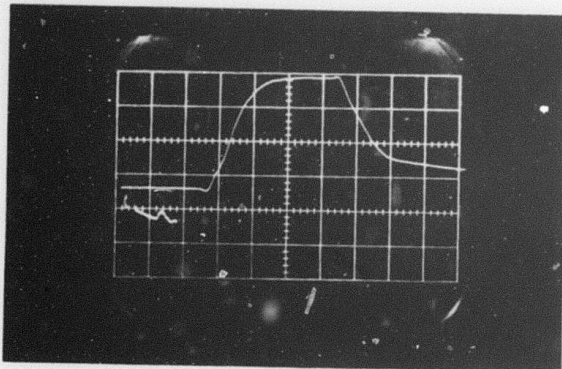


Figure 13 Reduced data from first uniaxial strain experiment in aluminum.



a. Carbon gages

Gage	Upper Radial	Lower Trans
Sweep rate	0.512	0.506 μ s /cm
Amplitude	1.049	1.000 V/cm
Bridge voltage	53.0	51.5 volts
Gage resistance	50.5	51.0 ohms



b. Manganin gages

Sweep rate	0.4903 μ s /cm
Amplitude	0.1932 V/cm
Bridge voltage	51.0 volts
Gage resistance	48.97 ohms

Figure 14 Recorded data from second uniaxial strain test in aluminum.

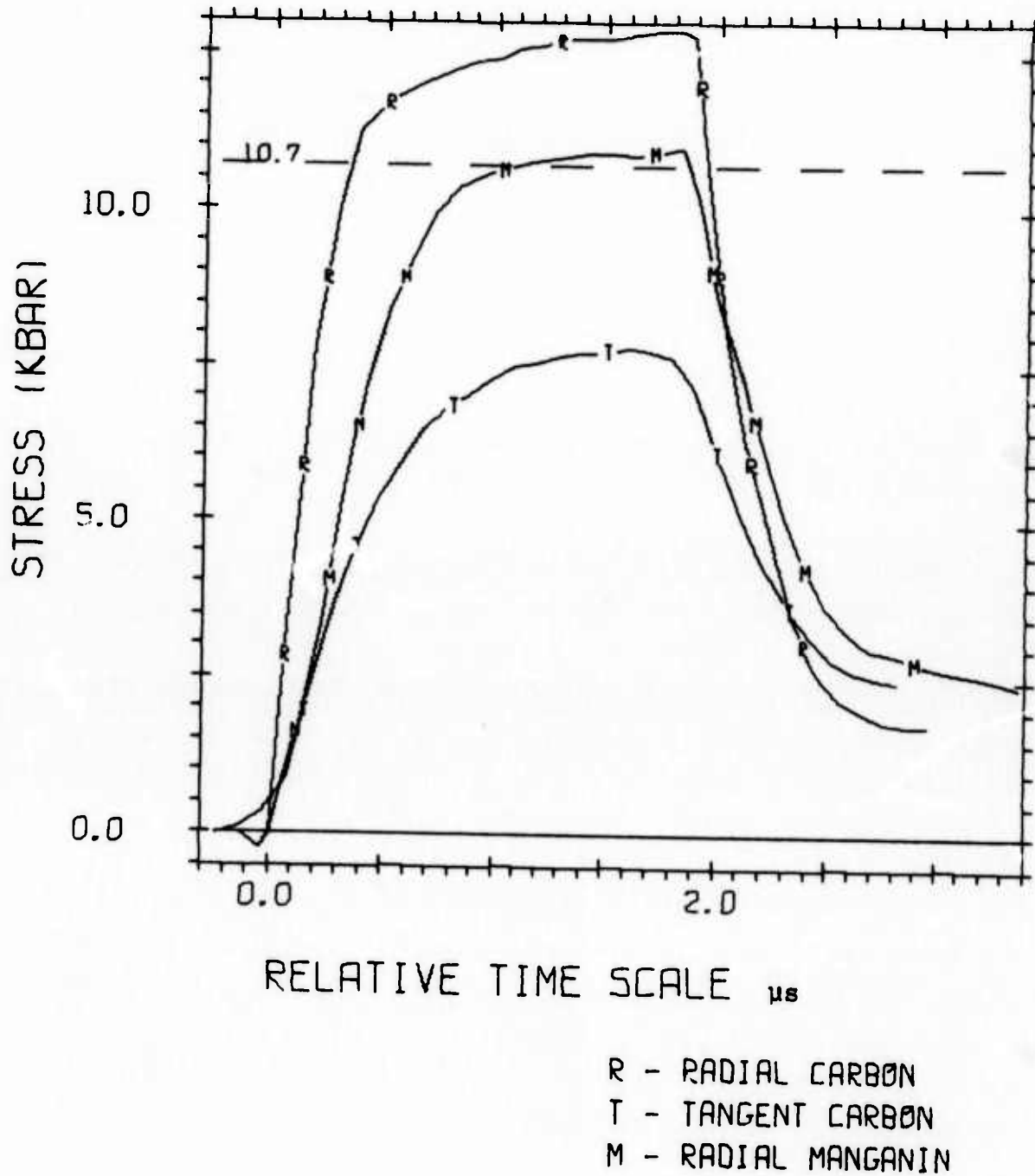


Figure 15 Reduced data from second uniaxial strain experiment in aluminum.

stress difference at the peak since the peak is held for a time sufficient for all gages to reach equilibration. For the first shot this difference is 2.7 ± 0.3 kbar. The assigned error is $\sqrt{2} \cdot \Delta\sigma$, with $\Delta\sigma$ being the average variation of the axial-mode gage stress from the value obtained from shock and particle velocities across the duration of the peak of the stress pulse. Based on a statistically significant sample of gage elements of similar construction to those used here, the expected deviation of a measurement from the calibration curve of Figure 16 is 6.5 percent (Reference 6).

Neglecting the axial carbon gage data of the second shot, for reasons outlined above, a stress difference of 3.0 ± 0.3 kbar is obtained at the peak stress.

These data are completely consistent with a constant value of 2.7 kbar quoted by Lundergan and Herrmann (Reference 9). Corroboration is offered by Barker (Reference 10). Erkman (Reference 11) has indicated the possibility that the yield strength increases slightly with pressure for 2024 aluminum. This situation, although not significant statistically, appears to be occurring here.

3.2.2 Westerly Granite. Observed in Figure 3 are three leads on the carbon gage element. With the center lead acting as ground, a single element can act as two independent gages. Until confidence had been gained on the two aluminum experiments, full use of the gage was not made; however, such caution was not exercised on the granite test.

The recorded data are displayed in Figure 17 while the reduced data are plotted in Figure 18. Data reduction proceeded via the use of resistance calibrations of the system and subsequent use of Equations 2 and 3.

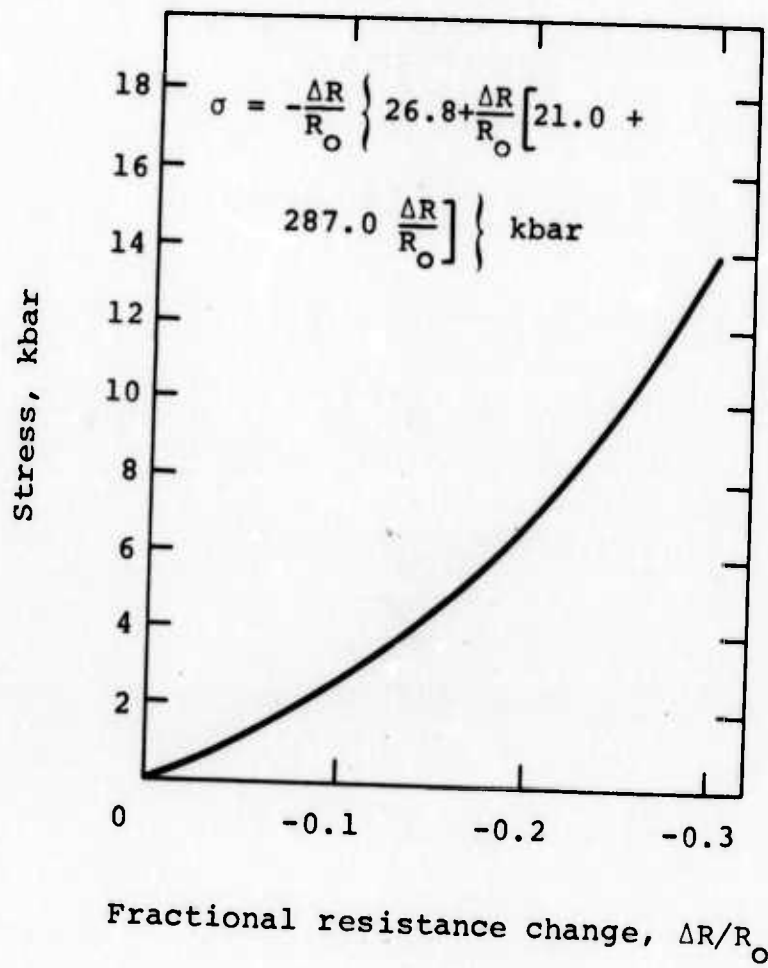
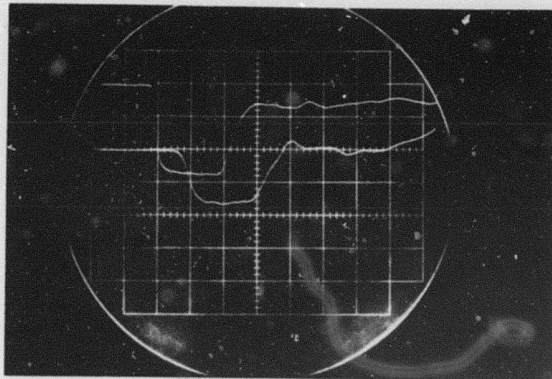
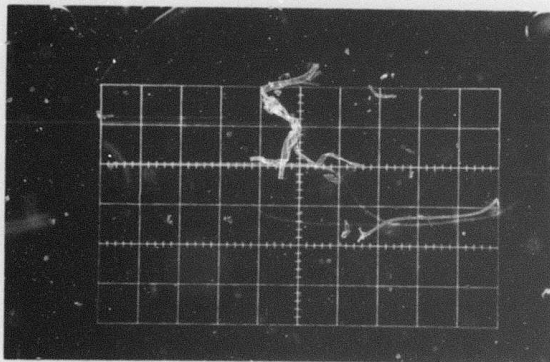


Figure 16 ETI carbon stress gage calibration (Reference 6).



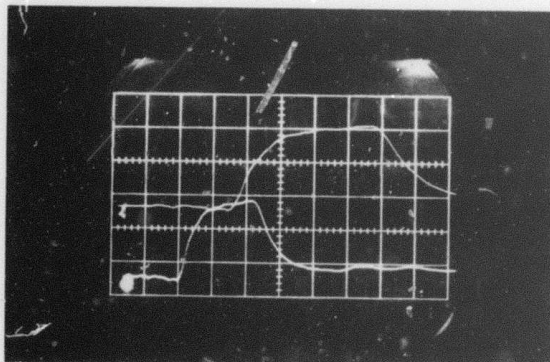
a. Carbon gages #1

Gage	<u>Upper</u> Radial	<u>Lower</u> Trans
Sweep rate	1.009	1.009 μs /cm
Amplitude	2.000	2.000 V/cm
Gage resistance	51.44	50.98 ohms



b. Carbon gages #2

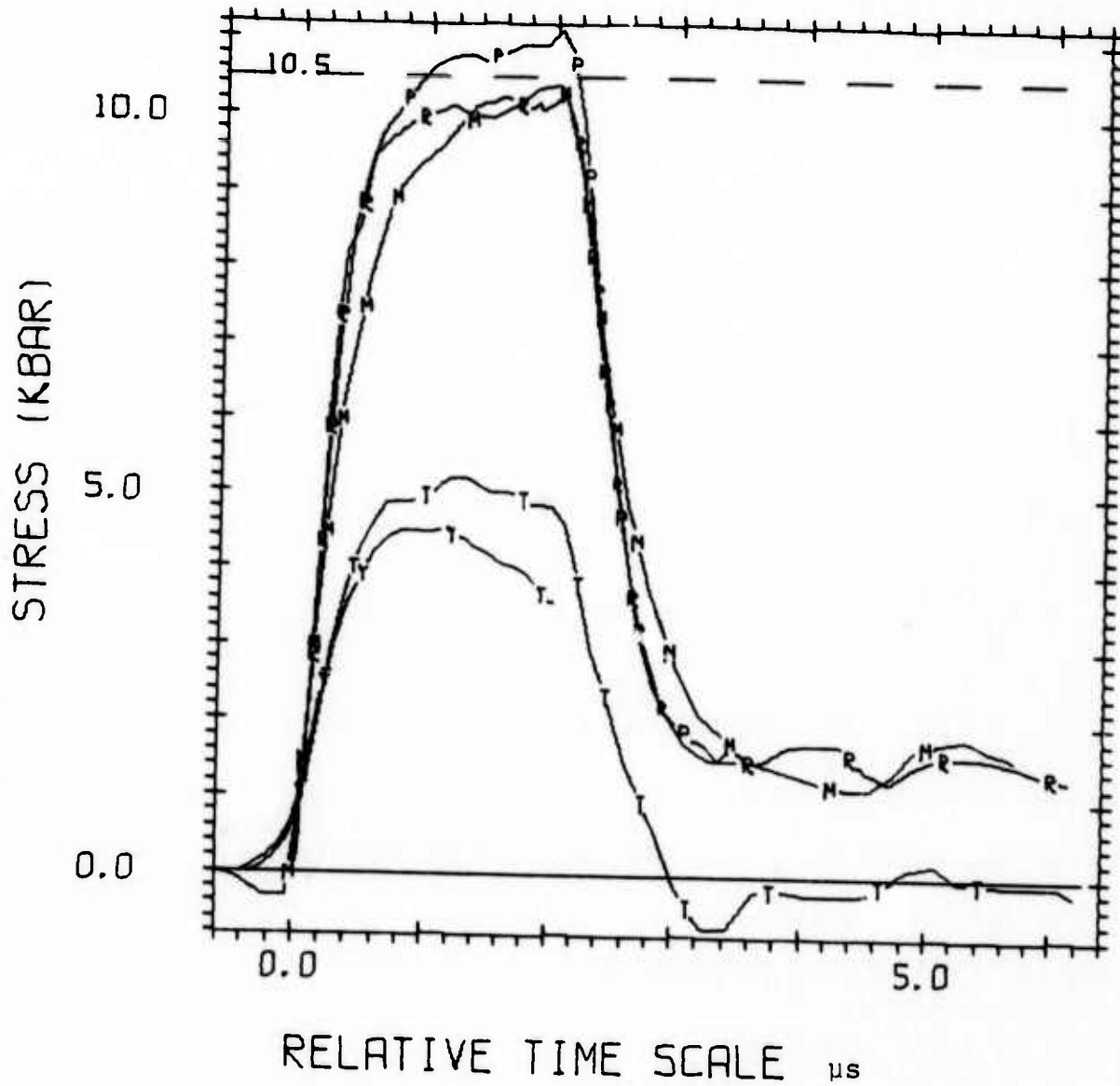
Gage	Radial	Trans
Sweep rate	0.504	0.500 μs /cm
Amplitude	2.000	2.000 V/cm
Gage resistance	48.99	52.87 ohms



c. Manganin gage (axial)

Sweep	<u>Lower Beam</u>
rate	0.9536 μs /cm
Amplitude	0.200 V/cm
Gage resistance	49.18 ohms

Figure 17 Recorded data from uniaxial strain experiment in Westerly granite.



R - RADIAL CARBON
 T - TANGENT CARBON
 M - RADIAL MANGANIN
 P - RADIAL CARBON
 Y - TANGENT CARBON

Figure 18 Reduced data from uniaxial strain experiment in Westerly granite.

Again, the risetime of the signal is too short for the transverse gage to follow, precluding any useful information regarding the stress difference during loading. The behavior of the axial mode gages is very like that predicted in Section 2, leading to the conclusion that the signal risetime may be even shorter than the response time of the axial mode gages. Considering this, only the data recorded at the peak stress are of use in determining the performance of the gages.

Correcting for a tilt between projectile and target of 1.03 mrad, the arrival time of the shock at the two components of the axial mode gage gives shock speeds of 5.9 and 6.3 mm/ μ s. Assuming the Hugoniot jump conditions to be valid, these yield axial stresses of 10.1 and 10.9 kbar respectively. Simmons and Brace (Reference 12) quote an average compressional velocity of 6.208 mm/ μ s at 10 kbar while Birch (Reference 13) reports a value of 6.23 mm/ μ s. (It must be noted that a simple average of all the data reported by Simmons and Brace is in precise agreement with Birch.)

Interestingly, the peak stresses recorded by the two axial mode carbon gages are in almost perfect agreement with the associated stresses calculated from shock speeds. As of this writing, such an occurrence can only be considered a coincidence.

The manganin gage rises to a maximum of 10.0 kbar (assuming a linear coefficient of 0.0025 kbar^{-1}) with a pulse to 10.5 kbar just prior to release. The anomalous behavior seen in the second aluminum shot is repeated here and, as will be explained in Appendix A, such a pulse should probably be ignored.

The transverse mode gages peak out at stresses of 5.0 and 4.6 kbar. Swanson (Reference 14) has shown that Westerly granite behaves elastically under these stress conditions (well below the failure surface), leading to a value of Poisson's ratio of $\nu \approx 0.31$ in good agreement with Walsh (Reference 15).

3.3 SUMMARY

Both in Westerly granite and aluminum the axial and transverse mode gages, as conceived here, behave very much as desired under dynamic uniaxial strain loading conditions.

Reference 6 has indicated the possibility of hysteresis in the carbon gage element with the resistance returning to its prestressed value upon complete release. As seen in Figure 18 when the axial stress releases to some non-zero value, both the carbon and manganin gages register the same stress level to within the experimental accuracy. If the manganin gage is presumed to be nonhysteretic the conclusion is that there is no evidence of hysteresis in the carbon element. Assuming the existence of some hysteresis in the manganin and a difference between the loading and unloading paths of carbon, such a conclusion is not absolute.

A summary of the pertinent experimental results is presented in Table 1. The stresses quoted are those measured at the peak. No estimate of the experimental error is quoted for the granite experiment, as the variance in data obtained from the two halves of each of the carbon gages may be taken as such an estimation.

TABLE I
EXPERIMENTAL RESULTS

Shot	Material	Projectile Tilt (mrad)	$2 U_p$ (mm/ μ sec)	U_s (mm/ μ sec)	$\rho_{O_2} U_s^2$ (kbar)	Manganin Axial (kbar)	Carbon Axial (kbar)	Carbon Transverse (kbar)
1	Aluminum*	1.00	0.077	5.8	6.01	----	6 \pm 0.2	3.3 \pm 0.2
2	Aluminum*	0.81	0.127	6.2	10.7	10.9	---	7.8 \pm 0.2
3a**	Granite [†]	1.03	0.131	5.9	10.1	10.0	10.1	5.0
3b**	Granite [†]	1.03	0.131	6.3	10.9	10.0	10.8	4.6

* Aluminum alloy (6061-T6).

** Same shot. Carbon gage data taken from both halves of gage element as independent gages.

[†] Westerly granite; Westerly, Rhode Island.

(a) Projectile velocity = $2 U_p$.

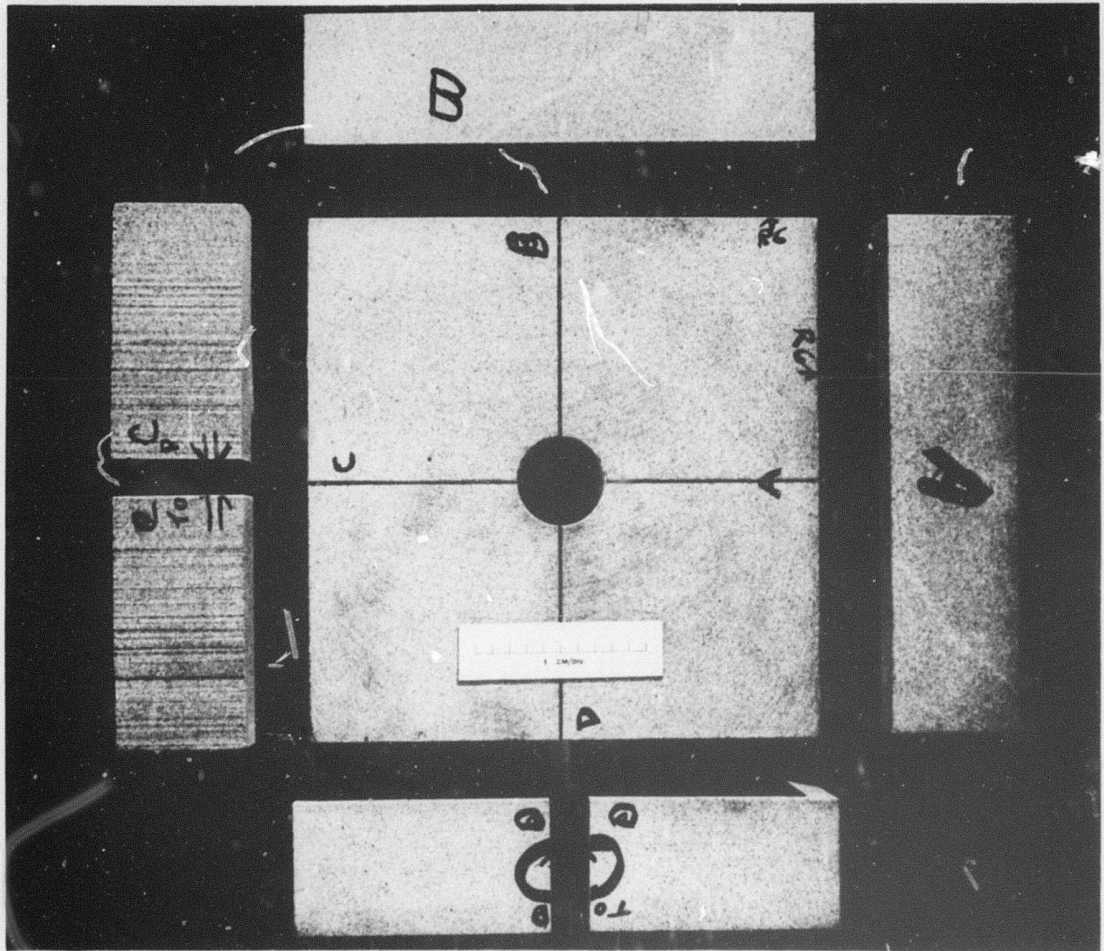
SECTION 4

SHOCK EXPERIMENT IN SPHERICAL SYMMETRY

4.1 PROCEDURES

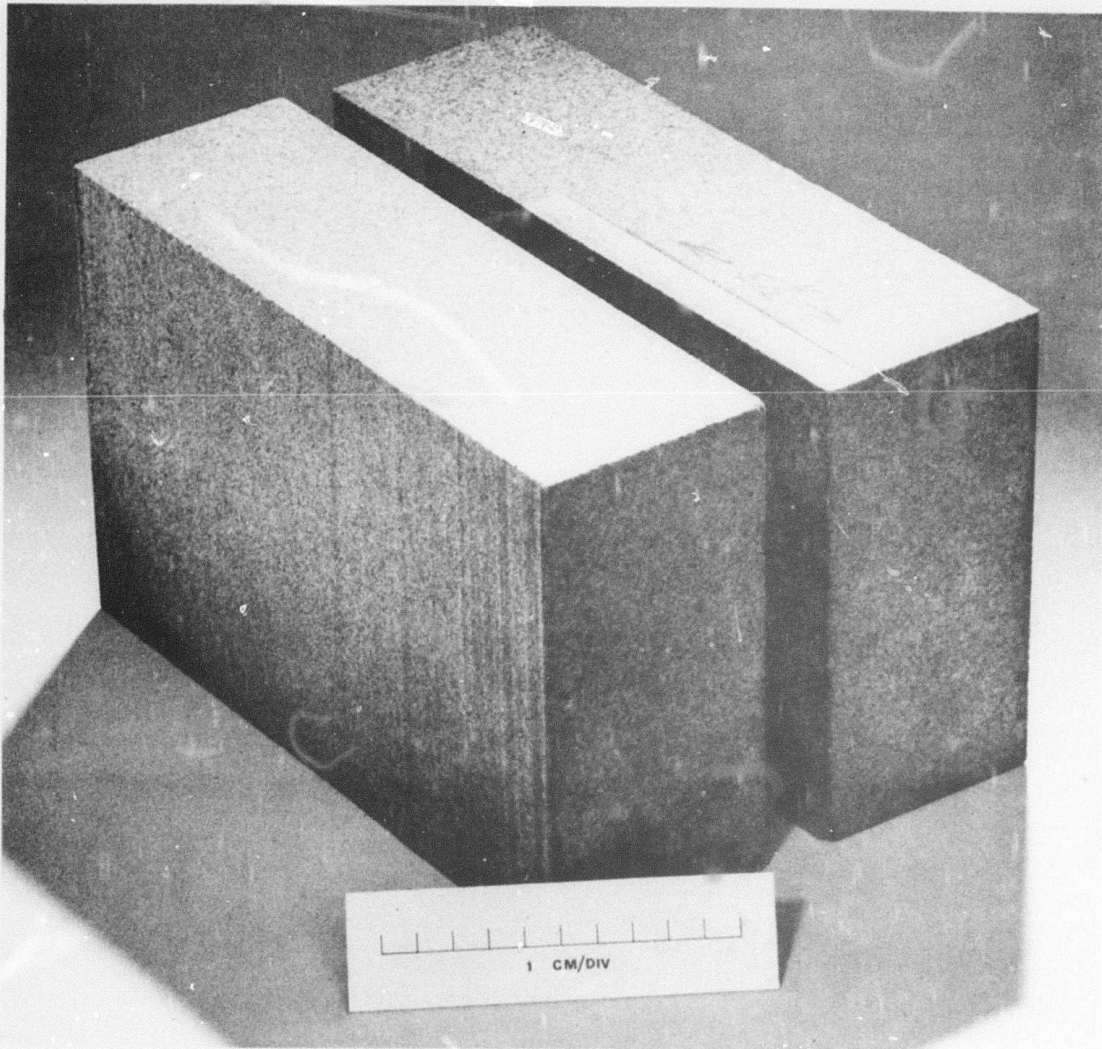
Figures 19, 20, and 21 show the various stages of assembly of the experiment. The base Westerly granite block was 12 x 12 x 10 inches and the backing plates were very nearly 3 inches thick. Figure 20 shows the $\frac{1}{2}$ inch by 0.012 inch deep slot ground to admit the tangential mode gage package. No such provisions were made for the radial mode gages. For backup, two radial gages and two tangential gage packages were installed at a radial position about 6 inches from the center of the charge. The explosive was a 1-inch-radius sphere of LX-04 emplaced at the center of the block and stemmed with the aluminum plug shown. The gages were mounted with respect to the charge such that spherical symmetry would be preserved. The assembled granite block was held together with Epocast 202 and D-40 hardener.

There were only two carbon element gages available and these were both installed in the tangential mode. As noted earlier, the elements were constructed so that each element could function as two independent gages; however, because of difficulty in bonding the carbon to polished sapphire, one of the two packages had effectively only a single gage. There was thus a total of three independent tangential gages installed. For the radial mode, manganin transducers of the type shown in Figure 2 were used. These were approximately 0.005 inch thick and were expected to be able to follow the rise of the shock front.



(73-6-7)

Figure 19 Preassembly "exploded" view of granite block for spherically symmetric experiment.



(73-6-19)

Figure 20 Split backing plate (side c) exposing slot to admit tangential gage.

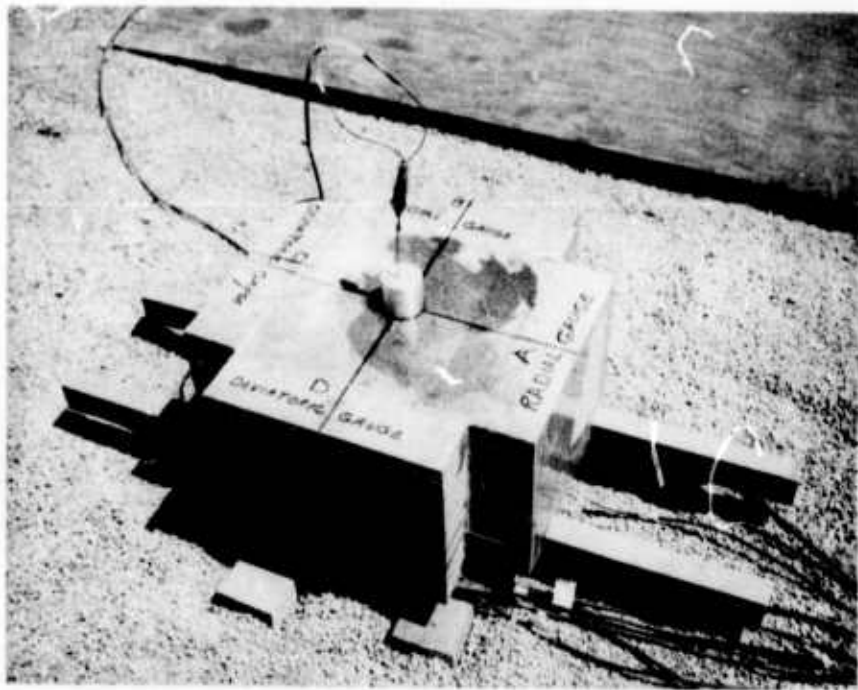


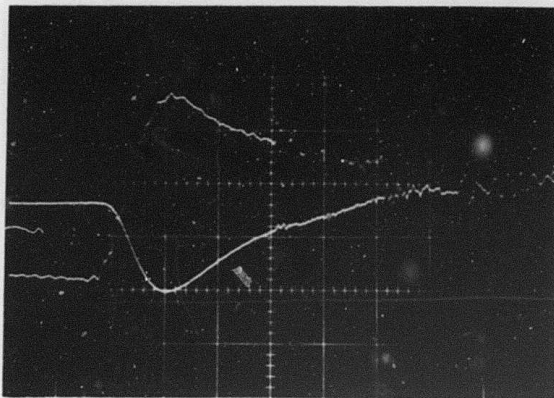
Figure 21 Final view of granite block immediately prior to experimentation.

Earlier work by Swift (Reference 8) using this type of manganin gage at the same radial position in Westerly granite indicated a risetime to peak stress of about 2 μ s. Not only should the radial (manganin) gages follow this, but also the tangential mode carbon element packages, which have a response time of about $\frac{1}{2}$ μ s as seen in the gas gun tests.

Data were again recorded on oscilloscopes. However, for this experiment, the impressed voltage across the bridge was carefully monitored, in addition to the imbalance voltage due to piezoresistance of each gage. Data reduction proceeded via use of the Wheatstone bridge equation (Equation 1) and external voltage and time calibration of the scopes used in the experiment. A calibration factor of 2.5×10^{-3} was assumed for the manganin. The loading calibration curve prescribed by Reference 6, with no provision for hysteresis upon unloading, was used to reduce the carbon gage data. These techniques are discussed in Section 3.1.

4.2 RESULTS

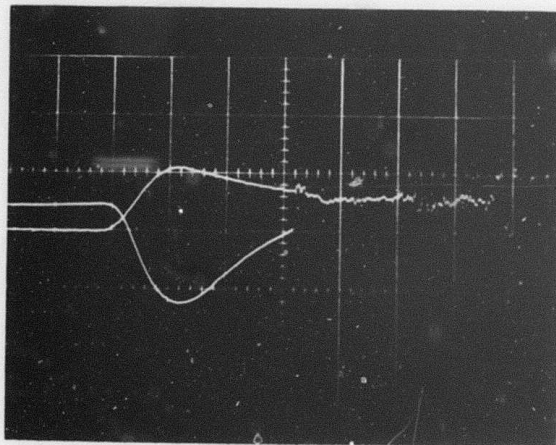
Figure 22 shows the recorded data while the reduced data are plotted in Figure 23. The radial manganin gage, MR-2, is plotted as a dashed line because the data are suspect: subsequent examination of the power supply showed that the channel for this gage had apparently been damaged during the experiment and this was the only gage for which there were no data from a bridge input voltage monitor. The dashed line represents the minimum stress amplitude attainable by MR-2, as estimated from the maximum voltage the charging capacitor C_1 (Figure 11) could hold.



a. Sides A and C

Gage	MR-1
Sweep rate	2.0014
Amplitude	0.2056
Bridge voltage	97.23
Gage resistance	48.34

CT-1	
1.9964 μs /cm	
0.9743 V/cm	
60.53 volts	
51.30 ohms	



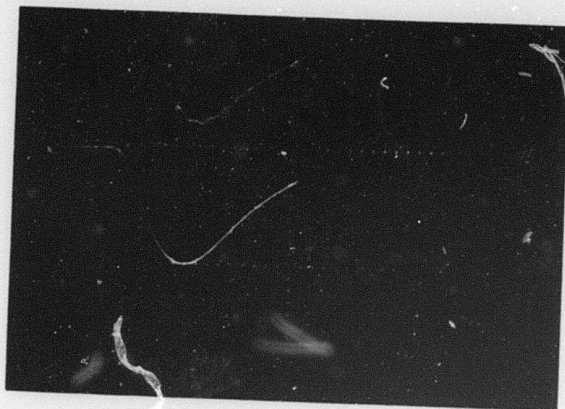
b. Sides B and D

Gage	MR-2
Sweep rate	2.0127
Amplitude	0.5054
Bridge voltage	<82.5
Gage resistance	48.29

CT-21	
2.0072 μs /cm	
1.0039 V/cm	
59.62 volts	
51.30 ohms	

Figure 22 Recorded data from spherical experiment in Westerly granite (positive resistance change is up) (page 1 of 2).

PIFR-393



c. Side D

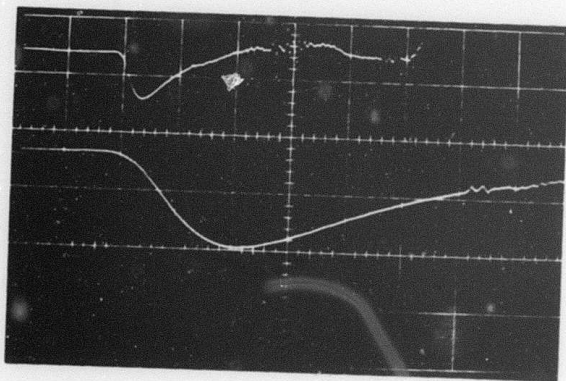
Gage
Sweep rate
Amplitude
Bridge voltage
Gage resistance

Lower

CT-21
1.9939
1.0167
59.02
51.10

Upper

CT-22
1.9968 μs /cm
0.8791 V/cm
54.29 volts
46.00 ohms



d. Gage CT-1

Sweep rate
Amplitude

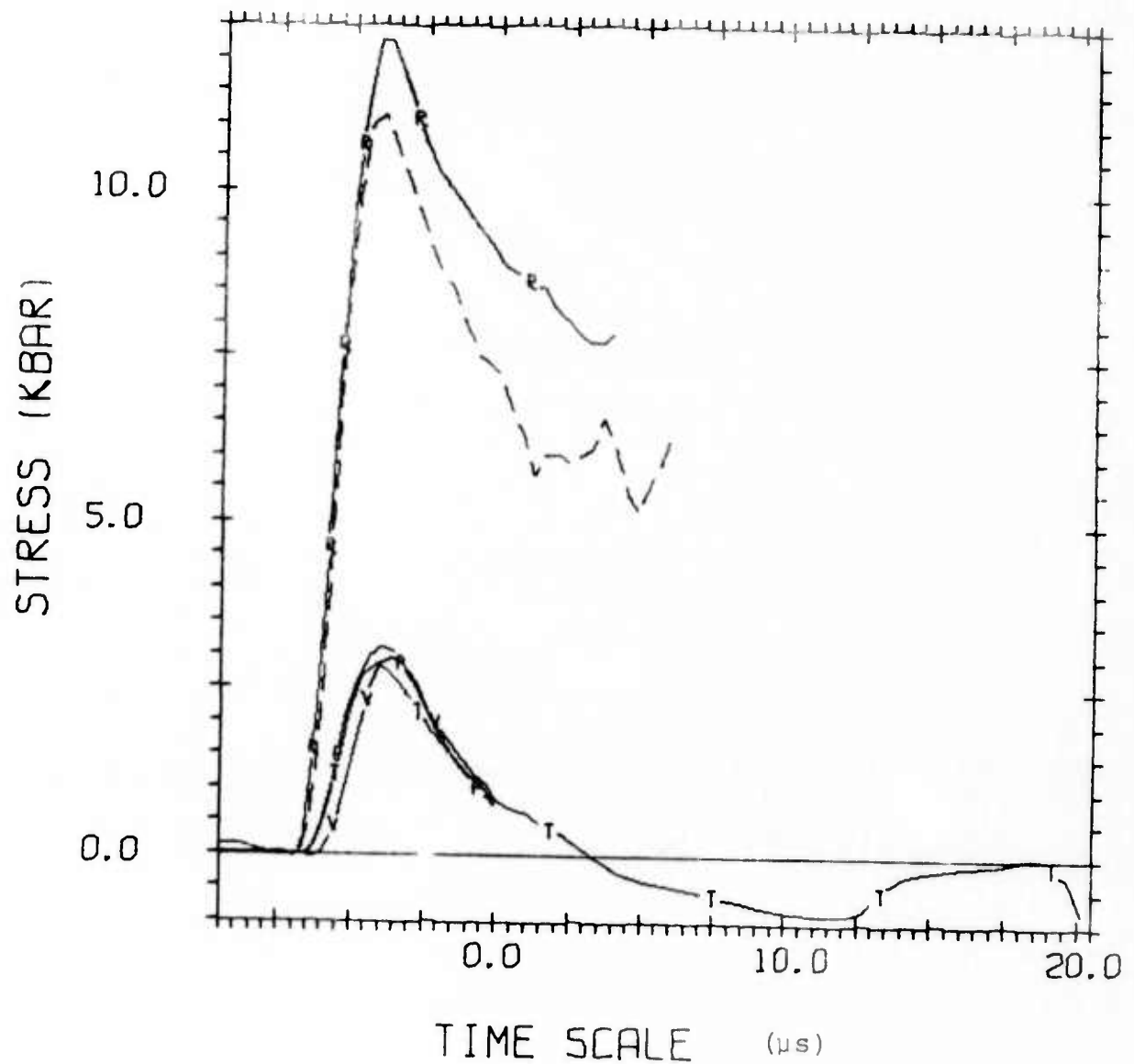
Lower

5
2

Upper

1 μs /cm
1 V/cm

Figure 22 Recorded data (page 2 of 2).



R - RADIAL MR - 1
 T - TANGENT CT - 1
 - - RADIAL MR - 2
 P - TANGENT CT - 21
 V - TANGENT CT - 22

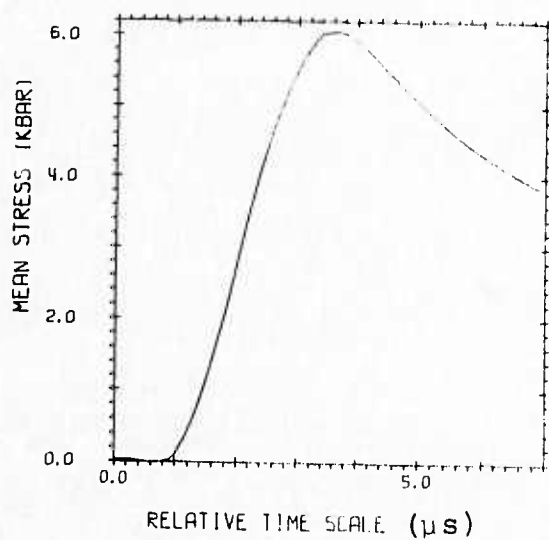
Figure 23 Reduced data from spherical experiment in Westerly granite.

Table 2 summarizes the experimental conditions and results of this experiment. The three carbon gages operating in the tangential mode registered peak stresses, which are within the ± 6.5 percent limit for variation indicated by Naumann.

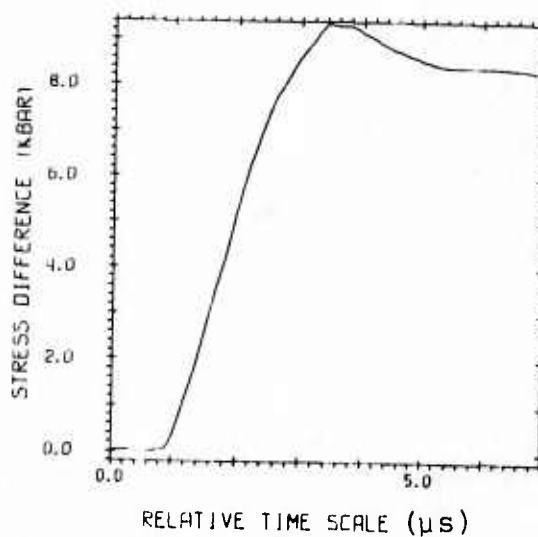
Gages CT-21 and CT-22 failed at the same time. These comprised two halves of the same carbon element, the two gages having a common vapor-deposited gold lead. The failure is strongly suggestive of the center (ground) lead failing, possibly due to a current overload. Since a similar failure was not observed in the uniaxial test, the mechanical failure of the lead cannot be ruled out. At any rate, this failure sent a signal through the entire system which was used as a time fiducial. The zero-time of Figure 23 is the time of occurrence of this failure and each gage record is adjusted accordingly. Data from times greater than zero are smoothed through the noise introduced by the gage failure and are not used in the subsequent analysis. As expected, the risetime of the radial stress is a bit greater than 2 μ s. Since the equilibration time of the tangential gages seen in the uniaxial tests is around 0.5 μ s, their ability to accurately follow the true tangential stress during the loading era is marginal. Under the two following, rather broad assumptions the stress deviator has been obtained:

- (1) Assume all gages are at the same radial position. Swift's data (Reference 8) indicate that the peak radial stress would be attenuated by no more than 3.5 percent over the entire radial span of the gage locations.
- (2) Assume the tangential gages faithfully represent the tangential stress during all phases of the stress wave.

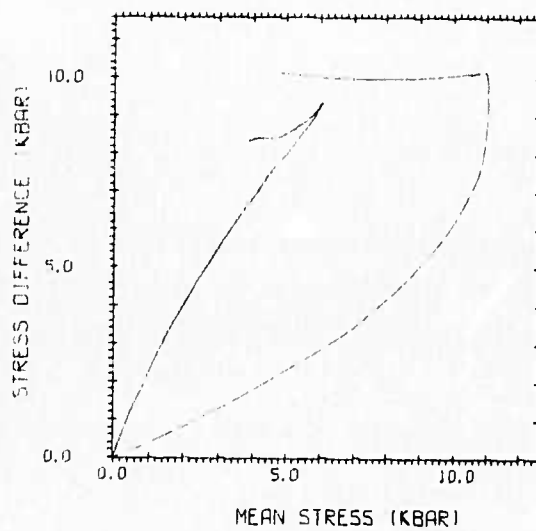
The calculation of the stress deviator proceeds as follows: The data represented in Figure 24 were made to have their arrival times identical by noting their respective radial positions,



a.



b.



c.

Figure 24 Stress histories and paths derived from Figure 23.

assuming a shock velocity of 6.23 mm/ μ s (Reference 13), and adjusting the time bases of the data accordingly. A mean tangential stress was obtained as a direct average of all three carbon gages and the corresponding radial stress was taken as that reported by MR-1; (MR-2 was not included for reasons detailed above). The analysis was not extended in time beyond the failure of the carbon gage package; the noise introduced in those gage records surviving precluded a meaningful stress deviator calculation.

4.3 DISCUSSION

Figures 24a, b, and c show the results of the analysis. Zero time is now arbitrary and has been chosen to be earlier than the earliest arrival of the stress wave. Superimposed in Figure 24c are the results of Grady's work (dashed) at a higher peak mean stress. Results obtained here are consistent with those of Grady; the slightly concave downward character of the stress-difference versus mean stress curve during loading is attributable to the frequency response of the tangential gage being different than that of the radial gage. In Reference 3 it was shown that digital filtering of all of the records to the frequency content of the gage having the lowest frequency response could lead to the correct data representation. Contractual limitations precluded this effort.

Some very interesting qualitative statements may be made from observations of the record of CT-1 displayed in Figure 22d. Assuming the gage does record the true tangential stress, this record indicates that Westerly granite can maintain a hoop tensile stress of greater than $\frac{1}{2}$ kbar for greater than 5 μ s. About 20 μ s after shock arrival there is a possible specimen failure. The tangential stress quickly returns to and stays at about zero for approximately 5 μ s. The distance from the

center of CT-1 to the outer surface of the backing plate is 2.814 inches. At a speed of 6.23 mm/ μ s the shock wave would require 23 μ s to reflect from this free surface and return as a tensile wave to the gage. The assumed velocity is appropriate for a stress wave of 10 kbar and is too high for lower stresses. The observed failure of the gage 25 μ s after the first arrival is almost certainly due to the reflected tensile wave from the free surface of the backing plate. Indeed, the character of the tangential gage record at +20 μ s (Figure 23) is that of the gage being driven into tension by the reflected tensile wave.

The granite block was epoxied with Epocast 202 and D-40 hardener. This combination is quoted as yielding a material with a tensile strength of 7500 psi; however, use at PI has indicated an unconfined tensile strength more on the order of 6000 psi or 0.41 kbar. This is about half the registered tensile hoop stress of the carbon gage.

Since the mean stress of the sample was probably still compressive at 2 kbar, it is not clear that the behavior occurring at +13 μ s in Figure 23 is a failure of the granite or of the epoxy bond (or for that matter that it represents any sort of failure). The fact that the gage returns to near zero "stress" between +15 and +20 μ s is strong evidence that this behavior is not an indication of gage stretching.

An additional caveat refers to the calibration of the carbon gage element. The bridge voltage data have been converted to stress through Equation 3, assuming the calibration is valid for both compression and tension. There is no experimental verification of Equation 3 for tension. The true magnitude of the hoop tension is thus unknown. Correlation does exist with previous experimental and theoretical work (Reference 16): failure of Westerly granite under cylindrically shock loaded conditions

was investigated. It was found that, based on the assumption that failure is determined by the hoop tensile stress, the tensile strength of competent Westerly granite is greater than 0.6 kbar and less than 1.5 kbar. It was further noted that cracks were propagated at a hoop tension of around 0.3 kbar. The untested calibration assumption leads to a tensile strength consistent with the above investigation.

All of these observations lend strength to the statement that the gage package designed in this work can operate effectively as a tangential stress transducer.

TABLE 2
EXPERIMENTAL RESULTS

<u>Gage</u>	<u>Material</u>	<u>Base Resistance (Ω)</u>	<u>Attached Resistance (Ω)</u>	<u>Orientation</u>	<u>Bridge Voltage (V)</u>	<u>Radial Position (cm)</u>	<u>Baseline Imbalance (divisions on scope)</u>	<u>Peak Stress (kbar)</u>
MR-1	Manganin	48.34	49.70	Radial	97.23	15.403	0	12.28
MR-2	Manganin	48.29	49.75	Radial	82.5*	15.458	+0.1061	11.2**
CT-1	Carbon	51.30	52.50	Tangent	60.53	15.555	0	2.861
CT-21	Carbon	50.10	51.45	Tangent	59.62	15.728	+0.2419	3.131
CT-22	Carbon	46.00	46.95	Tangent	54.29	15.928	+0.3699	2.964

* Not monitored: this is the maximum possible voltage.

** Minimum peak stress possible (derived from maximum bridge voltage).

SECTION 5

TECHNICAL REPORT SUMMARY

5.1 TECHNICAL PROBLEMS

Previous work (Reference 3) has shown the advisability of developing a gage that can directly measure stresses in a direction normal to the direction of propagation of a shock wave. Several authors have shown the theoretical possibility of obtaining the stress-strain path and stress deviators from measurements of only radial stress and velocity in spherical geometry (Reference 2). Such information has been obtained for the release portion of a stress wave in Westerly granite using a rather complete set of laboratory data (Reference 4). The technique used there may not be adequate for use upon field data from which one would extract the in-situ constitutive relations: circumstances beyond the scope of purely technical control often limit the number of gage stations on any given experiment and the quality (noise content, accuracy of gage placement, etc.) of the data returned is often not up to that produced in a laboratory environment. Under these conditions it may be difficult to calculate the tangential stress from measurements of only radial stress and motion.

Development of a gage to measure the tangential stress has been undertaken previously (Reference 5) with varying degrees of success. Two problems were encountered. The first was the uncertainty that the gage equilibrated to the correct stress level and the second arose from travelling shock interactions within the bonding surrounding the active gage material detracting

from the credibility of the gage. A two dimensional calculation was performed in Reference 5 to determine the equilibration of an element of circular cross section, indicating an equilibration time to the correct stress level of about 0.1 μ s. No solution of the Mach stem problem was demonstrated in the previous work.

5.2 GENERAL METHODOLOGY

Work on this contract proceeded in three discrete steps: Step 1, Gage Design and Computational Analysis; Step 2, Test of Design in Uniaxial Strain, Triaxial Stress Shock; and Step 3, Test of Design in Spherical Stress, Strain Shock. Based on the gage design successfully employed in Contract H0210015, simple calculations were performed to determine a limiting case to the equilibration time and stress. The gage is basically two thin layers of very high strength, high impedance material between which is sandwiched the active gage element. One-dimensional calculations using the Physics International 1DL finite difference code were performed assuming the active element to reside at a plane of symmetry (a rigid boundary). To simulate a tangential gage the test material, 2024 aluminum was uniformly loaded computationally to 6 kbar with the simulated bonder and gage package unstressed. The equilibration of the gage package was computed with this as a starting point.

Experiment work in Contract H0210015 showed the successful operation of the gage package design in a highly divergent, nearly hydrodynamic flow field. The next step undertaken in the present contract was to determine the behavior of the gage design in a high-strength, high-impedance material under conditions of uniaxial strain. Toward this end, three experiments were conducted via the projectile-impact technique using the Physics International 4-inch gas gun. In the first two tests, the gages

(one in the axial mode and the other in the transverse, or tangential, mode) were mounted in 6061-T6 aluminum. For the third test, the target and projectile material were Westerly granite.

The third and final step in the examination of the behavior of the gage was to test it in a high-strength, high-impedance material under conditions of spherical geometry. To effect this, a 2-inch-diameter sphere of LX-04 was detonated at the center of a 12 inch cube of Westerly granite. One stress gage was mounted on each of the four available faces such that manganin gages were used to obtain radial stress. Diametrically opposite each radial transducer, a gage package with a carbon element was mounted to obtain tangential stress.

In all the experiments the data were recorded on oscilloscopes. The gages were run as one leg of a standard Wheatstone bridge, an imbalance in voltage of which was the result of a change in resistance of the gage element. These data were subsequently digitized and processed.

5.3 TECHNICAL RESULTS

The simplified one-dimensional calculations indicate that the tangential gage under ideal conditions should reach an equilibrium at the proper stress within about 0.3 μ s. Large-scale, low-frequency oscillations observed in the careful two-dimensional calculation of Reference 5 were mitigated by the inclusion of the high-impedance laminate within the gage package. High-frequency, low-amplitude oscillations are superimposed on a lower frequency, more rapidly damped signal than that predicted in Reference 5. It must be remembered that the model of Reference 5 was a manganin wire imbedded in a 0.01-inch-thick layer of epoxy, which is quite a different concept from the gage package of this work.

Figures 13, 15, and 18 graphically display the results of the uniaxial strain experiments. Because of the very short risetime of the stress wave inherent in the impact (gas gun) technique, the data of greatest determinative value are the peak stresses: the transverse gage was not expected to, nor could it, follow the rise of the stress to its peak value. Because of the nature of the experimental technique, the maximum stress was maintained for a time sufficient for the system to come to equilibrium. Data obtained from these experiments are in excellent agreement with deviatoric stress information obtained by other workers for both 6061-T6 aluminum (References 9 and 10) and Westerly granite (Reference 12 and 13).

The data of Figure 23 show the behavior of the tangential gage in a spherically divergent flow field.

The risetime of the wave front was sufficiently long that the tangential gages could reasonably follow it. All three tangential gages gave very similar data, agreeing at the peak values to within about ± 4 percent of each other. It was pointed out that the best agreement that could possibly have been expected is about ± 3 percent, as the gages lay at slightly different radial positions from the explosive source.

Deviatoric stress data upon unloading are consistent with those derived by Grady (Reference 4). This reference considered data from a mean stress level which peaked around 11 kbar and obtained a constant (or nearly so) deviatoric stress of around 10 kbar upon unloading. In the current work, a peak mean stress of 6.1 kbar was attained with the release wave propagating at a nearly constant deviatoric stress of around 8.5 kbar.

Combining the evidence from the earlier experiments in a nearly hydrodynamic flow field, uniaxial strain tests in aluminum and Westerly granite and the spherically divergent experiment in Westerly granite lead to the conclusion that the gage employed here can accurately measure tangential stress, under the proper conditions.

5.4 DOD IMPLICATIONS

Of great current interest to the DoD is the general subject of stemming and containment. Many suggestions have been proffered as how best to effect containment based on several differing conceptions as to the bulk failure mechanisms of the containment material. Paramount is the requirement of a reasonably accurate estimate of the constitutive properties of the in-situ material, including its failure surface. One of the areas of interest is the effect of water pore pressure: can it decrease the stress attenuation while simultaneously lowering the failure surface? An operative tangential stress gage would yield hard, experimental data on this point.

Other related applications in the scope of computational prediction of mining operations are also evident.

5.5 IMPLICATIONS FOR FURTHER RESEARCH

The gage concept has been successfully demonstrated in the laboratory under three widely varying conditions:

- a. Large spherically divergent flow-in, low-impedance, low-strength materials.
- b. Uniaxial strain shock in high-strength, high-impedance materials.
- c. Spherically divergent flow in a high-strength, high-impedance, geologic material.

To show the universal validity of the gage system concept, it is necessary to test it in an actual field operation.

Below 20 kbar the piezoresistive carbon gage developed by ETI is quite satisfactory. There are several areas of additional investigation of gage properties required, however. First, reasonably strong evidence was seen that the gage could measure tensile stresses. The material (carbon phenolic) has not been calibrated in tension. This should be done. Second, only rudimentary information is available on the difference between the loading and unloading paths taken by the material. This should also be made a high-priority item.

REFERENCES

1. Gene Simmons and Amos Nur, Granites: Relation of Properties In-Situ to Laboratory Measurements, Science, 162 789, 15 November, 1968.
2. Richard Fowles and Roger F. Williams, Plane Stress Wave Propagation in Solids, J. Appl. Phys. 41 360, January 1970.
3. T. F. Stubbs, Determination of the Dynamic Constitutive Properties of In-Situ Material, PIFR-311, Physics International Company, April 1972.
4. D. E. Grady, J.G.R. 78, 1299, March 1973.
5. M. W. McKay and C. S. Godfrey, Study of Spherically Diverging Shock Waves in Earth Media, DASA 2223, Physics International Company, March 1969.
6. W. J. Naumann, Carbon Stress Gage Handbook, CR-72-101, Effects Technology, Inc., October 1972.
7. E. Barsis, E. Williams, and C. Skoog, Piezoresistivity Coefficients in Manganin, J. Appl. Phys., 41 5155, December 1970.
8. Robert P. Swift, The Dynamic Response of Westerly Granite to Spherical Stress Waves, PIFR-146-3 (DASA 2717), Physics International Company, August 1971.
9. C. D. Lundergan and W. Herrmann, J. Appl. Physics, 34, 2046, July 1963.
10. L. M. Barker, Fine Structure of Compressive and Release Wave Shapes in Aluminum Measured by the Velocity Interferometer Technique, SC-DC-66-2447, Sandia Laboratories, Albuquerque, preprint.
11. J. O. Erkman, Elastoplastic Effects in the Attenuation of Shock Waves, Fourth Symposium on Detonation, Vol. 1, p. 383, October 1965.

REFERENCES (cont.)

12. Gene Simmons and W. F. Brace, *J.G.R.*, 70, 5649, November 1965.
13. Francis Birch, *J.G.R.* 65, 1083, April 1960.
14. S. R. Swanson, Development of Constitutive Equations for Rocks, doctoral dissertation, University of Utah, December 1969.
15. J. B. Walsh, *J.G.R.* 70, 5249, October 1965.
16. J. E. Reaugh, I. O. Huebsch, and R. P. Swift, Fracture and Comminution of Rock, PIFR-310, Physics International Company, November 1972.

APPENDIX
ANOMOLIES SEEN IN MANGANIN GAGES

The risetime seen in the manganin gages is much greater than would be expected of the actual shock front. Additionally both Figures 14b and 17c indicate an opposite polarity hump immediately preceding both the arrival of the loading wave and the unloading wave. This effect is not observed in the axial mode carbon gages.

It will be remembered that the manganin gage on the first of the aluminum tests was inoperative so that the first occurrence of this effect was in the second experiment. Since, at that time, there was no clear explanation for the occurrence, no changes in the manganin gage were made for the third and final gas gun experiment, conducted in Westerly granite. The behavior persisted, though it was not so clear-cut.

During the construction of the targets there were slots milled to admit the carbon gage packages. These were approximately 0.012 inch deep and 0.5 inch wide and ran the full length of the backing portion of the targets (Figure 10). Only about half of the slot was occupied by the carbon gage; the other half was used for the manganin axial mode gage. In order to have the gage read as close to the true stress as possible, an aluminum shim approximately 0.01 inch thick was intended to be placed in the slot along with the manganin gage (which is about 0.002 inch thick). Unfortunately there was no shim stock available of this thickness; so two layers of thinner material were used. It was recognized only after the experiments that what had been built was a device having two thin conductors in close proximity to an electrically active element (the manganin gage), and insulated from it by the epoxy bonder. This is, in effect, a rather lossy inductor-capacitor combination. One would expect a back-emf to be generated by the foil due to a change in the current to the wires of the gage resulting qualitatively in the observations actually made. The situation is analogous to a

Preceding page blank

low-pass filter existing in the circuit. Figure A-1 depicts the results of processing the first quarter of a sine wave having a frequency w_0 with a low-pass digital filter having a cut-off frequency of $3 w_0$. The initial downward pulse is an affectation of the filter and should be disregarded as should the pulse at the top of the wave.

This was clearly a problem generated by the overdesign of the system. The situation could have been corrected by either of two mutually exclusive actions. First, the gage could have been installed without a shim, the gap being filled with epoxy. The gage would probably have "rung" about the peak stress with a period governed by the transit time of sound across the 0.012 inch of epoxy. The other solution would be to have used a dielectric shim approximating the properties of the aluminum more closely than did the epoxy. A simple, inexpensive, and readily available item is microscope slide coverglass.

SPECIAL LOW PASS OF FIRST QUARTER WAVE

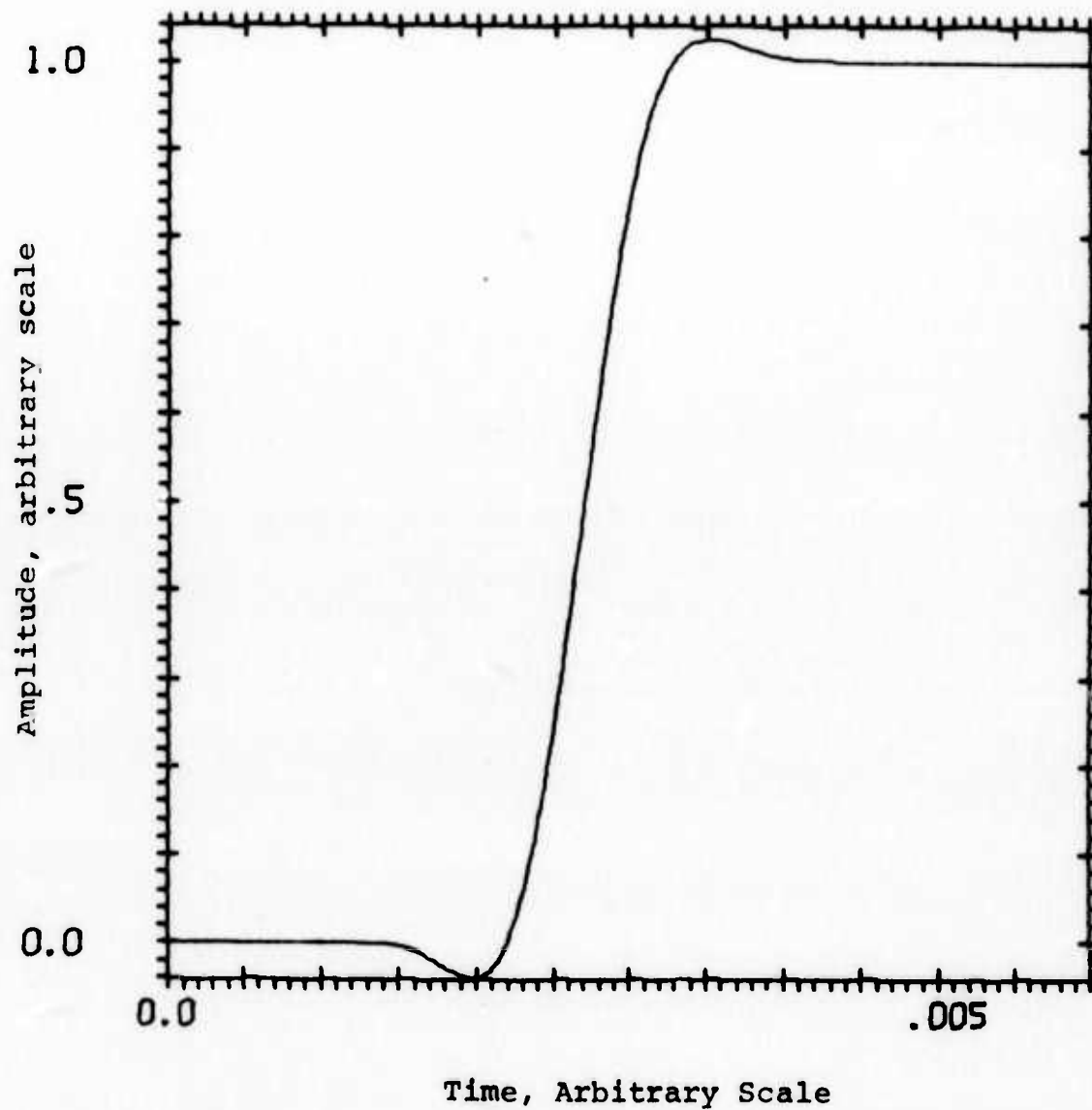


Figure A-1 Results of low pass digital filtering a quarter sine wave of frequency ω_0 at the cut-off frequency $3\omega_0$.